MIDDLE EAST TECHNICAL UNIVERSITY
FACULTY OF ENGINEERING
ELECTRICAL ENGINEERING DEPARTMENT

DETERMINATION OF ANTENNA FAR-FIELD RADIATION-PATTERNS FROM NEAR-FIELD DATA

Submitted to the Faculty of Engineering
in partial fulfillment of the requirements for the Degree of Doctor of Philosophy in Electrical Engineering

by

TUNCAY BİRAND

Approved by:

Ankara, Turkey

August, 1971

ACKNOWLEDGEMENT

The author wishes to acknowledge with great gratitude the supervision, many helpful suggestions and constant encouragement of his supervisors Assoc.Prof.Dr. A. Marinçiç and Prof. Dr. Y. Tokad.

Special thanks are due to Asst.Prof.Dr. A. Hızal for many valuable discussions.

The author received scholarship from TUBITAK (Türkiye Bilimsel ve Teknik Araştırma Kurumu - Turkish Scientific and Technical Research Council) since March 1969. He is, therefore, much indebted to this organization.

The author is also thankful to Asst.Prof.Dr. H. Oranç and Mr. A. Fer for the valuable discussions in the early phase of the work and to Asst.Prof.Dr. C. Toker for his constant encouragement.

Thanks are due to the workshop staff (specially to Mr. İ. Talı, Mr. N. Altınoğlu and Mr. G. Balta) for the help they offered in realizing various parts of the measurement set-up.

Miss. H. Özer, for the accurate and swift typing of the thesis and Mr. A. Fındıkçıoğlu, for producing the drawings, are greatly acknowledged.

ABSTRACT

In this thesis a new method, based upon integral equation solution is developed for the prediction of far-field radiation patterns of optically large antennas from near-field measurements.

A general formula of transmission between two antennas is derived using the concept of angular spectrum of plane waves and Brown's generalized reciprocity theorem.

It is shown that, in the application of the well known Fourier transform method of radiation-pattern determination, the error produced by neglecting the directivity of the measuring probe can be corrected by a simple and rigorous method described in this thesis.

The technique of antenna synthesis is presented and an integral equation is obtained whose solution yields the far-field radiation-pattern. It is shown that, if the near-field measurements are performed employing the antenna synthesis technique, then the spatial filtering action of the synthesized pattern reduces the computational work needed in pattern prediction considerably. The phase factor in the integrand also contributes to the filtering action of the synthesized pattern.

The solution to the integral equation is obtained by expanding the unknown angular spectrum function into an orthogonal series making use of the sampling theorem. Thus, the problem of solving the integral equation is converted into the problem of simultaneous solution of a set of linear algebraic equations.

For the detailed numerical study of errors in the solution of integral equation, a digital computer (IBM 360) is utilized.

The theory presented in this thesis is tested experimentally by predicting various H-plane far-field radiation-patterns. The experimental results reveal a very good agreement between the direct-measured and predicted far-field patterns.

TABLE OF CONTENTS

LIST OF PRINCIPAL SYMBOLS

α_j, β_i	=	angles defining orientation of transmitting antenna
j, i	=	indices defining orientation of transmitting antenna
ϕ_m, θ_n	=	angles defining orientation of receiving antenna
m, n	=	indices defining orientation of receiving antenna
j	=	$\sqrt{-1}$
$\bar{k}$	=	propagation vector
$\bar{r}$	=	position vector
Y_o	=	characteristic admittance of free space (in mho's)
$\rho_d = \ell$	=	distance between the transmitting antenna and the measurement plane (in cms)
λ	=	wavelength (in cms)
x,y,z	=	cartesian coordinate variables defined w.r.t. the transmitting antenna
x',y',z'	=	cartesian coordinate variables defined w.r.t. the receiving antenna
η , ξ , ρ	=	cartesian coordinates of the fixed coordinate system
s_1, s_2, c	=	direction cosines defined w.r.t. (x,y,z) system
s_1', s_2', c'	=	direction cosines defined w.r.t. (x',y',z') system
D_{ij}^{mn}	=	signal received by receiving probe whose orientation w.r.t. the fixed coordinate system is designated by the indices m,n. Indices i,j define the orientation of transmitting antenna
$D(\beta_i), D_{ij}$	=	response of synthesized antenna
$c_n, c_{nm}^x, b_{nm}^x, b_{nm}^y$	=	complex coefficients in sampling expansions
$h_m(s_1)$, $g_n(s_2)$	=	functions in sampling expansions
A	=	normalization constant for signal in waveguide of feed system of receiving antenna

I. INTRODUCTION

In this thesis the determination of far-field radiation-patterns of antennas with large aperture size to wavelength ratio (optically large) are considered.

In order to measure the far-field pattern of an antenna, the measurements have to be performed at so called Rayleigh distance. This distance is given by $2a^2/\lambda$ ([COL 1], Ch.2), where a and λ, stand respectively, for the maximum linear dimension of the antenna and the free space wavelength.

As it is well known, Rayleigh distance for some optically large antennas can be so large that it may be very difficult if not impossible to find a proper test site. In such cases, one of the ways of measuring far-field patterns is to employ radio-astronomical antenna pattern measurement methods which are based on the utilization of extraterrestial bodies as radio emission sources [KUZ].

Several investigators have worked on the problem of determining antenna far-field radiation patterns from measurements made in the near and Fresnel zones of the antenna.

The methods in the literature which enable the determination of far-field radiation-patterns from measurements made at smaller distances than the Rayleigh distance, fall into one of the two main categories below;

(i) direct methods that provide direct measurement of the far-field patterns at distances smaller than the Rayleigh distance,

(ii) indirect methods that base upon the processing of the data obtained from near or Fresnel zone measurements to determine far-field patterns.

Methods such as focusing, utilization of metal lenses for plane wave generation fall into the first category whereas the methods of Fourier transformation, mode expansion, etc. fall into the second category.

Woonton et.al. [WO 1] have experimentally shown that, by utilizing a metal microwave lens, the nearly spherical wavefront generated by a waveguide opening can be converted into an approximate plane wavefront and then the E-plane far-field pattern of a horn placed in the plane wave region can be measured by rotating it around its aperture center. In this method, to obtain accurate results, the metal lens need be considerably larger than the aperture dimensions of the antenna being measured. For this purpose the method is suitable to make indoor pattern measurements of some primary feed antennas for which laboratory pattern measurements are inconvenient to perform. Afterwards various errors arising in the utilization of the method were studied [WO 2].

Bickmore [BIC 1] developed a focusing criterion for antennas whose aperture planes can be molded about a spherical surface. Later he showed that the far-field patterns of the class of antennas mentioned above can be measured in the Fresnel region by means of focusing. Thus the usual minimum distance requirement could be reduced from $2a^2/\lambda$ to about $0.1a^2/\lambda$ where a stands for the maximum linear dimension of the aperture of the antenna whose far-field pattern is intended to be measured [BIC 2].

Another method of focusing is based upon displacing the primary feed radiator of the reflector type antennas from the focus along reflector axis [BRA] , [TSE] . Braude and Yesepkina derived relations which permit the determination of the minimum admissable distance at which it is possible to measure far-field pattern with a prescribed error. Their focusing method was developed for parabolic reflectors [BRA] . They also pointed out that due to the impossibility of obtaining accurate focusing, phase errors are generated which can be of decisive importance.

Tseytlin [TSE] considered the effect of amplitude changes in the reflector aperture field due to primary radiator off-setting to accomplish focusing, and the effects of the directivities of the primary radiator and the measuring probe.

A classical method of obtaining far-field patterns of aperture antennas from near-field measurements is taking the Fourier transform of the aperture electric field distribution [RAM] . In this method various errors can be introduced if the directivity of the measuring probe is not considered and if the interaction between the probe and the antenna is large. It may be very difficult to make measurements at the apertures of some types of antennas owing to the presence of the feed-systems, etc. Sometimes a precise aperture definition may not exist.

A method of accounting for the directivity of the measuring probe is given in this thesis (See [BIR 1]).

The method introduced by Hamid is based upon taking the Fourier transform of the autocorrelation function of the aperture electric field distribution which yields the far-field power pattern [HAM] . As the transverse near-field is pointed out to fall off rapidly, the measurements were performed on a finite region of a plane parallel to the aperture of the measured antenna.

His method is restricted, since in his investigation the aperture field distribution is considered as real and seperable. The directivity of the measuring probe was not taken into account.

In Kern's method, which accounts for the directivity of the measuring probe, far-field pattern is obtained by taking the Fourier transform of near-field data measured on a plane parallel to the aperture of the antenna whose pattern is to be estimated [KER 1] . For practical reasons, measurements are performed over a finite region of the transverse plane and therefore the results obtained are approximate. The order of the approximation depends upon how rapidly the transverse field decays exterior to the region within which the measurements are carried out. In an other publication which utilizes this theory, results of experimental work giving the far-field pattern of an optically large horn lens and a standard gain horn were reported [KER 3] .

Bates and Elliott derived the Fresnel region pattern as a function of the far-field polar-diagram [BAT] . Then making certain simplifying assumptions connected with the form of the polar-diagram, they have shown how to estimate the true sidelobe levels of long broadside arrays from Fresnel region measurements. Application of their theory requires apriori knowledge of the width of the main-beam, between its zeros, which can be approximately determined from measurements in the Fresnel region. The method resulted after the assumptions made about the form of the far-field pattern is an approximate one and is applicable only to arrays whose patterns satisfy certain requirements.

Martsafey showed that a quasi-plane wave can be synthesized at the aperture of a measured antenna, by means of a single probe-radiator which travels over a plane surface to synthesize a large planar array [MART] . In other words, a probe-radiator can be

moved to various positions to describe a planar space lattice and then the responses of the measured antenna, corresponding to various radiator positions, can be summed up to obtain the response of the antenna to an incident quasi-plane wave. The idea utilized in his work is similar to the idea of producing a quasi-plane wave by the utilization of a metal lens [WO 1], but differs in the way of achieving it. It is pointed out that, in order to determine the radiation pattern in any plane, a knowledge of a single set of responses of measured antenna corresponding to all radiator positions in the space lattice is adequate, and that the data corresponding to rotations of the measured antenna can be generated from that set by giving proper phase shifts to the individual responses. But of course, this argument is valid only approximately, since the amplitude of the field of the synthesized array varies with the rotation of the synthesized wave's wave-front [MART]. In this method, the directivity of the probe-radiator is not considered. It should be noted that a true-plane wave would be generated only if the synthesized array was of infinite extent.

Brown's method in which the radiated field is expanded in a series of radially expanding modes, consists of determining a number of unknown complex coefficients of the expansion which are also shown to correspond to the unknown coefficients in the series expansion for the far-field radiation pattern [BR 1]. These coefficients can be calculated from a Fourier analysis of the near-field data. In order to account for the directivity of the measuring probe the so called "response constant" need be evaluated. Brown's analysis was for a two dimensional system.

Martin applied Brown's two dimensional theory to determine the far-field pattern of a line source antenna having seperable aperture distribution [MAR]. The measurements were performed

at the far-field of one aperture dimension and in the near-field of the other. Comparison of predicted and direct measured far-field patterns were given. Agreement over the main beam was good but became less over the sidelobe regions. As it can be clearly seen from the investigation of the two and three dimensional transmission equations of Jull (Eq. 10 [JUL 1]) and Brown (Eq. 28,[BR 2]) respectively, the two dimensional theory will not give the same receiving probe response as the three dimensional one. Thus, utilization of cylinderical mode expansion in three dimensional systems, for radiation pattern estimation, is actually an approximation.

Jull [JUL 2] developed a series expansion for the near-field pattern of an antenna measured with a directive probe from a cylinderical-mode expansion of the radiated field. First three terms of the expansion containing the far-field pattern and its derivatives were inverted to yield the far-field pattern in terms of the near-field pattern and its derivatives. The accuracy of the method was theoretically checked for an assumed cosine aperture distribution of the measured antenna. It is pointed out that small errors in near-field measurements may lead to very large errors in the derivatives causing the predicted pattern to be inaccurate.

Some of the described methods were observed to have the disadvantage of being applicable to only restricted classes of antennas. The results obtained by the utilization of some of the more general indirect methods are also bound to be approximate as the predicted patterns are obtained from a process of a limited near-field data. The limitidness of the integration limits in the methods basing upon transform techniques and the truncation of the series in mode expansions are the causes of some severe errors.

The results obtained by using any of these methods share the property of yielding far better results around main-beams centered at zero degrees, than the results in sidelobe regions.

In this thesis using the concept of angular spectrum of plane waves ([BO] , [CL] ,[COL 1] ,[ST]) a transmission formula is derived. This formula gives the expression of the signal in the waveguide of a probe antenna illuminated by a radiating one making use of Brown's general reciprocity theorem [BR 3] . The derived formula is the more general form of Browns transmission equation (Eq. 24 [BR 2]), and is valid for arbitrary positionings and any kind of aperture electric field polarizations of the transmitting and receiving antennas. The general transmission equation is then used to develop a correction method for the errors which arise in the Fourier transform technique [RAM] of far-field prediction due to receiving probe directivity.

It is proved that the response of a large array can be synthesized by making a number of amplitude and phase measurements over a plane surface. Then an integral equation involving the unknown angular spectrum functions (which correspond to far-field pattern under certain conditions [BOO] , [CL]), phase factor, pattern of synthesized antenna and measurement values is obtained. The solution of that integral equation is obtained by expanding the unknown spectrum functions in series of orthogonal functions by making use of the sampling theorem.

It is known that the angular spectrum function determining the far-field pattern and the aperture electric field distribution are Fourier transform pairs [CL] , [BOO] , [COL 1] .

On the other hand, for optically large aperture antennas, the transverse field on the aperture plane decays very rapidly away from the radiator [COL 1] . Thus, with very little error the

aperture electric field distribution can be considered to be limited in space. Therefore the Fourier transform pair of this "space limited" function can be expanded in a sampling series. Once the complex coefficients of this expansion are evaluated, the far-field pattern can be easily obtained. By the orthogonal function expansion of the unknown, the solution of the integral equation is converted into the solution of a set of simultaneous algebraic linear equations whose solution is enforced at a discrete number of measurement values. A number of integrals whose integrands are composed of known functions need be evaluated. For this purpose a digital computer is utilized. Through the use of a set of linear equations which are written in matrix form, the coefficients are obtained by matrix inversion. The minimum number of terms in the sampling expansion is determined by the largest optical size of the measured antenna.

The pattern of the synthesized antenna introduced into the integrand of the integral equation by the measurement method provides an angular filtering action [BIR 2] , [BIR 4] enabling the reduction of the original integration limits. Thus the necessary computational work can be considerably reduced.

The individual orthogonal functions of the sampling expansion are of decaying nature. Hence the neglection of the tails of the truncated terms will give rise to very small errors for small angles. Aperture synthesis technique, due to its filtering action further assists to this truncation error minimization for small angles.

The integral matrix is defined to be the matrix which is composed of integrals with known integrands. The diagonal entries of the integral matrix can be made considerably larger than the off-diagonal entries of the same row by a pre-selection of the angular positions of the measured antenna. In applications to fanned-beam antennas it is shown that

some off-diagonal entries can be taken equal to zero without much affecting the mean-percent error in the predicted patterns [Ch. IV, Table 4.1]. In the prediction of radiation patterns of optically very large antennas, the inversion of very large matrices will be required. The computation of the inverse integral matrix is simplified considerably if a number of off-diagonal entries could be considered as zero [TOK].

The accuracy of the integral equation solution for fanned-beam type antennas is checked by computer simulation. The results for the assumed cosine aperture distribution are much more accurate compared to the results obtained by Jull [JUL 2].

The method is proven experimentally by predicting the patterns of various fan-shaped patterns. Aperture blockings were used to produce different H-plane patterns. Comparison of predicted and direct measured patterns are given. The results obtained are very satisfactory.

It is important to note that the same integral matrix, which is computed for an antenna of specific optical-size, can be utilized in the prediction of the far-field patterns of smaller optical-size antennas as well. This is due to the fact that the integral matrix is not dependent upon the measurement values. However the integral matrix is determined by the charadteristics of the synthesized and receiving antennas and the geometry associated with the problem. Hence, provided that measurements are performed utilizing a specific measuring probe, and that the seperation between the measured and the synthesized antennas is kept fixed, the same integral matrix can be utilized for antennas whose optical sizes lie in a certain range.

Of course, although the integral matrix computed for a very large optical-size antenna may be employed for an antenna with a much smaller optical-size, it is not necessary; since utilization of an integral matrix of smaller size will suffice the purpose.

Neither the methods presented in the literature, nor the present theory given in this thesis account for the effect of multiple reflections which may be present between the measured and measuring antennas. However, in the present method, the measurements can be performed at distances at which this interaction problem can be made negligible and the far-field pattern, with the same accuracy can be obtained.

II. TRANSMISSION BETWEEN TWO ANTENNAS

2.1. Plane Wave Spectrum Representation of Electromagnetic Fields and the Relation between Angular Spectrum and Far-Field Radiation Pattern

It is known that the solution to the wave equation in a source free region can be represented as an angular spectrum of plane waves which primarily is an integral type of representation of the solution to Maxwell's equations [BO] , [ST],[COL], [BOO], [KER 2], [CL]. In this kind of representation, the source that gives rise to the electromagnetic field is taken to be an electric planar current sheet and electric or magnetic field distribution over a suitably chosen plane.

To represent the field at any point in space, the plane waves travelling in all directions are superposed after each one is multiplied by an appropriate complex weightening factor which is a function of the propagation direction. In three dimensional coordinate systems, direction cosines are used to specify the directions of propagation and in two dimensional coordinate systems it is usually more convenient to use angles directly. Therefore, in order to express the electromagnetic field, the general vectorial expression of the plane wave, after being multiplied by a weightening function called the "angular spectrum function", is integrated over all angles or direction cosines. For the complete representation of the field, it is however necessary to integrate the general vectorial expression over the complex angles. By this integration one obtains the "evanescent waves". No energy is propagated by the evanescent waves. These waves just represent an exponential decay of the field as one moves away from the source

[BOO], [CL], [BO]. On the other hand, if there exists a harmonic time dependence, then the integration is only over the direction cosines. However for representing fields having arbitrary time dependences , it is also necessary to integrate over all frequencies[ST].

From the above introductory remarks, it can be easily seen that, to specify the field, first the angular spectrum function is to be determined. This is achieved by expressing the surface source distribution as a Fourier integral. Then the "angular spectrum function" happens to be the Fourier transform of the planar source distribution. The source distribution can be resolved into tangential components over the source plane and furthermore an angular spectrum function can be associated with each component. If the source is an electric surface current sheet, then two independent tangential component of the electric or magnetic current densities are sufficient to determine the angular spectrum functions. If, on the other hand, the source is of the form of an aperture distribution, then the angular spectrum functions may be associated with the tangential components of either $\bar{E}$ or the $\bar{H}$ field over the aperture plane. However, in some diffraction problems a linear combination of the electric and magnetic surface current densities should be utilized to determine the angular spectrum functions[CL].

If the source distribution is a localized one, then at sufficiently large distances from the source, a radiation field (or far-field) may be defined. At the radiation zone, the distance and angular dependences become seperable; i.e., $\bar{E}_{rad} \propto \frac{e^{-jkr}}{kr} \bar{F}(\theta,\varphi)$. $\bar{F}(\theta,\varphi)$ is the vectorial far field radiation pattern of the source. Using the "stationary phase" method of integration, the above form of the radiation field can easily be obtained from the angular spectrum representation of the electromagnetic field provided that the conditions

(i) $kr \gg 1$ and (ii) $r \gg D$ are satisfied. In condition (ii), D stands for the maximum linear dimension of the source. Hence, for planar source distributions that are confined to a finite area in space, the angular spectrum function is also equal to the far-field radiation-pattern. On the other hand, for infinitely extending aperture distributions, the concept of radiation field fails as the far-field conditions cannot be satisfied. But even then, the angular spectrum concept is applicable, and an angular spectrum function can exist which will have a singularity.

One must note that $\bar{F}(\theta, \varphi)$ is a vectorial spectrum. It consists of a combination of the spectrum functions associated with the transverse components of the aperture field distribution. Therefore, in practical applications, as the source distributions are considered to be localized in space, in the solution of antenna problems, a knowledge of two independent spectrum functions is sufficient to specify the far-field radiation patterns.

2.2. Derivation of the Transmission Formula between Two Antennas of Arbitrary Aperture Electric Field Distributions

2.2.1. Representation of the Electromagnetic Field in Terms of Spectrum Functions

Usually microwave antennas are aperture type antennas. Hence it is more convenient to determine angular spectrum functions using two of the tangential components of the aperture electric or magnetic field. Referring to Fig.2.1, if $E_x(x, y)$ and $E_y(x, y)$ are the x and y components of the aperture electric field, respectively; being consistent with Clemmow's normalization [CL], one has

$$F_x(s_1, s_2) = \frac{1}{\lambda^2} \int_{-\infty}^{\infty}\int_{-\infty}^{\infty} E_x(x, y)\, e^{jk(s_1 x + s_2 y)}\, dxdy \qquad (2.1)$$

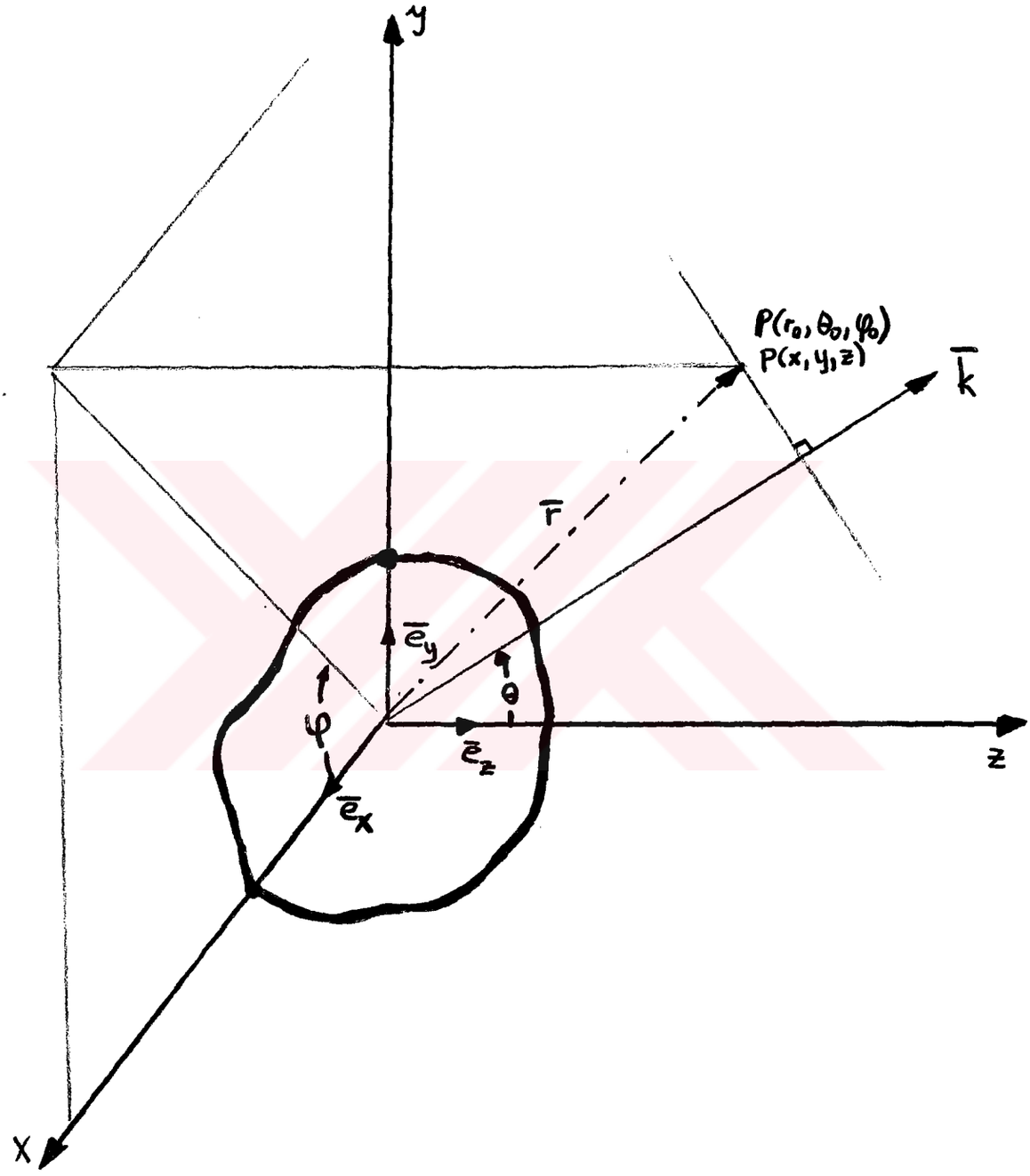

Fig. 2.1 Radiating Aperture

$$F_y(s_1, s_2) = \frac{1}{\lambda^2} \int_{-\infty}^{\infty}\int_{-\infty}^{\infty} E_y(x, y)\, e^{jk(s_1 x + s_2 y)}\, dxdy \qquad (2.2)$$

where $F_x(s_1, s_2)$ and $F_y(s_1, s_2)$ denote the angular spectrum functions associated with the x and y components of aperture electric field distribution and s_1, s_2 stand for the direction cosines. As the time dependence is harmonic, phasor notation will be used to represent the fields. In region $z > 0$, $F_x(s_1, s_2)$ and $F_y(s_1, s_2)$ are the spectrum functions that are responsible for the x and y components of the electromagnetic field. The third field component follows through the use of Maxwell's equations.

A spectrum function $F_z(s_1, s_2)$, associated with the z-component (normal component) of the aperture electric field may also be defined. Again, from Maxwell's equations $F_z(s_1, s_2)$ can be determined from a knowledge of F_x and F_y.

If any component of the aperture electric field is identically equal to zero, then the same component is zero everywhere in region $z > 0$. [BR 2].

As Eqs. 2.1 and 2.2 imply, the angular spectrum functions $F_x(s_1, s_2)$ and $F_y(s_1, s_2)$ are defined to be equal to the Fourier transforms of the x and y components of the aperture electric field distribution respectively.

For the complete representation of the electromagnetic field in region $z > 0$, six components associated with the $\bar{E}$ and $\bar{H}$ fields should be specified. Two of the spectrum components were associated by the x and y components of the aperture $\bar{E}$-field. Then the spectrum functions for the other four components will follow from Maxwell's equations. The three components of the electric field in region $z > 0$ can then be expressed as follows:

$$E_x(x,y,z) = \int_{-\infty}^{\infty}\int_{-\infty}^{\infty} F_x(s_1,s_2)\, e^{-jk\,[s_1x+s_2y+cz]}\, ds_1 ds_2 \qquad (2.3)$$

$$E_y(x,y,z) = \int_{-\infty}^{\infty}\int_{-\infty}^{\infty} F_y(s_1,s_2)\, e^{-jk\,[s_1x+s_2y+cz]}\, ds_1 ds_2 \qquad (2.4)$$

$$E_z(x,y,z) = \int_{-\infty}^{\infty}\int_{-\infty}^{\infty} F_z(s_1,s_2)\, e^{-jk\,[s_1x+s_2y+cz]}\, ds_1 ds_2 \qquad (2.5)$$

in which $c = \sqrt{1-s_1^2-s_2^2}$ and these expressions are consistent with Clemmow's normalization factor [CL]. The components F_x and F_y are determined from Eqs.2.1, 2.2 and F_z will follow from the relation $\bar{\nabla}.\bar{E} = 0$. The components of $\bar{H}$ are obtained from $\bar{\nabla}x\bar{E} = -jw\mu\bar{H}$. This derivation is given in Appendix I. Thus, with ; $\exp\,[-jk(s_1x+s_2y+cz)] = \exp\,[-j\bar{k}.\bar{r}]$, the $\bar{E}$ and $\bar{H}$ field in region $z > 0$ are expressed as:

$$\bar{E}(x,y,z) = \int_{-\infty}^{\infty}\int_{-\infty}^{\infty} \left[cF_x\bar{e}_x + cF_y\bar{e}_y - (s_1F_x+s_2F_y)\bar{e}_z\right] e^{-j\bar{k}.\bar{r}}\, \frac{ds_1 ds_2}{c} \qquad (2.6)$$

$$\bar{H}(x,y,z) = Y_o \int_{-\infty}^{\infty}\int_{-\infty}^{\infty} \Big\{\left[-s_1s_2F_x-(1-s_1^2)F_y\right]\bar{e}_x + \left[(1-s_2^2)F_x+s_1s_2F_y\right]\bar{e}_y$$

$$+ \left[cs_2F_x+cs_1F_y\right]\bar{e}_z\Big\}\, e^{-j\bar{k}.\bar{r}}\, \frac{ds_1 ds_2}{c} \qquad (2.7)$$

2.2.2. The Formula for Determining the Received Signal

In Fig.2.2, the antenna T is assumed to be the transmitting antenna whose $\bar{E}$ and $\bar{H}$ fields, respectively, at any point P in space, are given by Eqs. 2.6 and 2.7.

The transmission equation between the transmitting antenna T and the receiving antenna R can be derived by making use of Brown's generalized reciprocity theorem [BR 3].

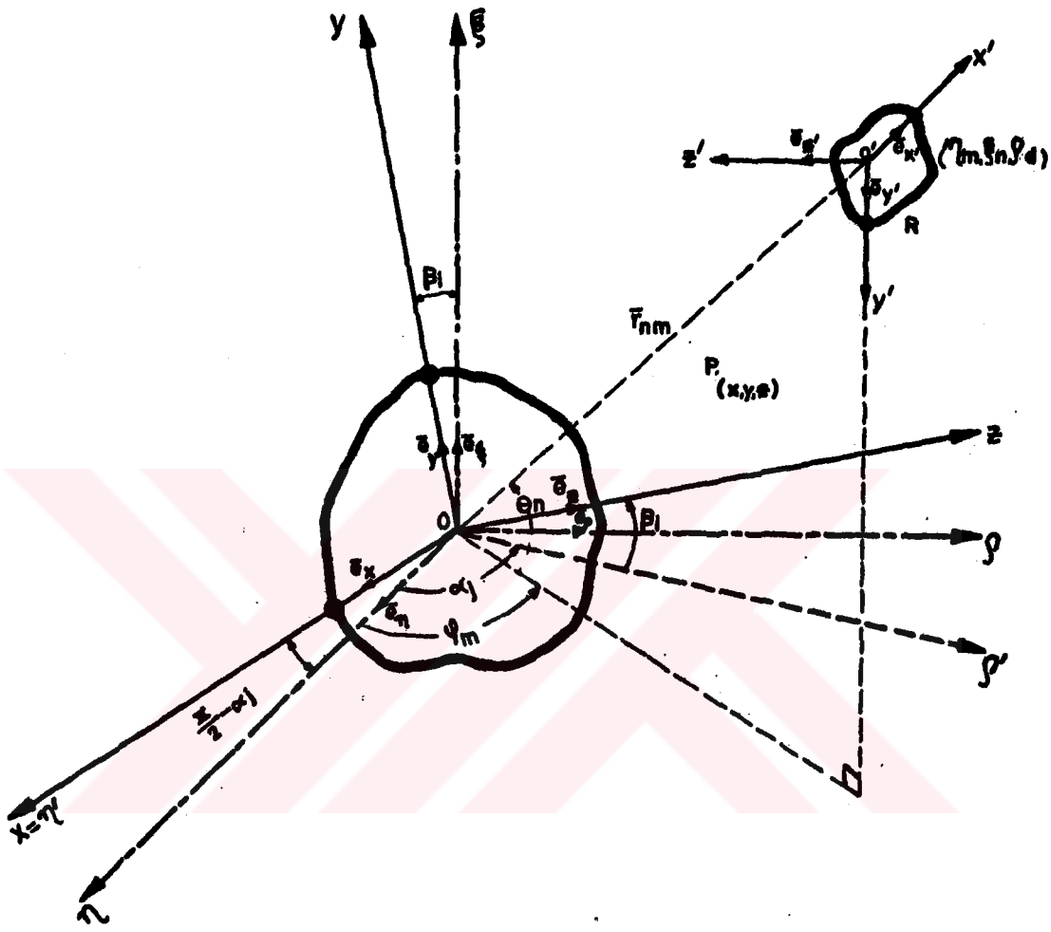

Fig:2.2 Coordinate systems associated with the transmitting and receiving antennas

The complex amplitude of the received signal D, at a reference cross section in the waveguide of the receiving antenna R, when illuminated by a plane wave, is given by;

$$D = \frac{Y_o A e^{-j\frac{\pi}{2}}}{k} \; \bar{E}_o(\bar{r}').\bar{F}^R(s_1', s_2') \qquad (2.8)$$

A is a normalization constant defined in reference [BR 3].
$\bar{E}_o$ is the electric field of the incident plane wave expressed w.r.t the (x'y'z')-system
$\bar{F}^R(s_1',s_2')$ is the vectorial angular spectrum function of antenna R expressed w.r.t (x'y'z') system

It should be noted that in the expression of D the dot product of the incident field and the vectorial spectrum appears. This implies that the receiving antenna R does not accept the waves that are incident in directions in which $\bar{F}^R$ does not have a component.

In order to derive the general transmission formula, first any plane wave defined in xyz-system must be expressed in the x'y'z'-system. Then in order to account for the contribution of all plane waves that are considered to form the general electromagnetic field, integration must be carried out over all these plane waves, each of which is weighted by a proper angular spectrum function.

2.2.3. Expression of the Electric Field Radiated by Antenna T w.r.t x'y'z'-system

From Eq. 2.6, the electric field at a point P(x,y,z) in region $z > 0$, which is due to a plane wave travelling in a direction specified by the propagation vector $\bar{k}$, caused by a general aperture distribution of antenna T, can be expressed as:

$$\bar{E}_o(\bar{r}) = \left[F_x(s_1,s_2)\bar{e}_x + F_y(s_1,s_2)\bar{e}_y - \frac{1}{c}(s_1F_x + s_2F_y)\bar{e}_z \right] e^{-j\bar{k}.\bar{r}} \qquad (2.9)$$

where $\bar{r} = \bar{e}_x x + \bar{e}_y y + \bar{e}_x z$ is the position vector in xyz-system.

Referring to Fig.2.2unit vectors in (x,y,z) and (η,ξ,ρ) systems are related as;

$$\begin{bmatrix} \bar{e}_x \\ \bar{e}_y \\ \bar{e}_z \end{bmatrix} = [R] \begin{bmatrix} \bar{e}_\eta \\ \bar{e}_\xi \\ \bar{e}_\rho \end{bmatrix} \tag{2.10}$$

where $[R]$ is the rotation matrix given by;

$$[R] = \begin{bmatrix} \sin\alpha_j & 0 & -\cos\alpha_j \\ -\sin\beta_i\cos\alpha_j & \cos\beta_i & -\sin\beta_i\sin\alpha_j \\ \cos\beta_i\cos\alpha_j & \sin\beta_i & \cos\beta_i\sin\alpha_j \end{bmatrix} \tag{2.11}$$

and simple relations exist between the unit vectors in (η,ξ,ρ) and (x',y',z') systems;

$$\bar{e}_\eta = \bar{e}_{x'} \ , \quad \bar{e}_\xi = -\bar{e}_{y'} \ , \quad \bar{e}_\rho = -\bar{e}_{z'}$$

Substituting these relations in Eq. 2.10, we have

$$\begin{bmatrix} \bar{e}_x \\ \bar{e}_y \\ e_z \end{bmatrix} = [R] \begin{bmatrix} \bar{e}_{x'} \\ -\bar{e}_{y'} \\ -\bar{e}_{z'} \end{bmatrix} \tag{2.12}$$

Since the direction cosines s_1, s_2 and c are the components, respectively, of the unit propagation vector $\frac{\bar{k}}{|\bar{k}|}$ on x, y and z axes, the matrix $[R]$ also governs their transformation; i.e.,

$$\begin{bmatrix} s_1 \\ s_2 \\ c \end{bmatrix} = \begin{bmatrix} R \end{bmatrix} \begin{bmatrix} s_1' \\ -s_2' \\ -c' \end{bmatrix} \tag{2.13}$$

The relation between x,y,z and x',y',z' consists of a rotation plus translation which can be expressed as;

$$\begin{bmatrix} x \\ y \\ z \end{bmatrix} = \begin{bmatrix} R \end{bmatrix} \begin{bmatrix} x'+\eta_m \\ -y'+\xi_n \\ -z'+\zeta_d \end{bmatrix} \tag{2.14}$$

Then $\bar{E}_o(\bar{r})$ in Eq.2.9 can be expressed in x'y'z'-coordinate system to read;

$$\bar{E}_o(\bar{r}') = \left[b_{x'}\bar{e}_{x'} + b_{y'}\bar{e}_{y'} + b_{z'}\bar{e}_{z'} \right] e^{-jk\left[s_1 x + s_2 y + cz\right]} \tag{2.15}$$

where

$$b_{x'} = F_x(s_1,s_2)\left(\sin\alpha_j - \frac{s_1}{c}\cos\beta_i\cos\alpha_j\right) - F_y(s_1,s_2)\left(\sin\beta_i\cos\alpha_j + s_2\cos\beta_i\cos\alpha_j\right) \tag{2.16a}$$

$$b_{y'} = F_x(s_1,s_2)\left(\cos\alpha_j + \frac{s_1}{c}\sin\beta_i\right) + F_y(s_1,s_2)\left(\frac{s_2}{c}\sin\beta_i - \cos\beta_i\right) \tag{2.16b}$$

$$b_{z'} = F_x(s_1,s_2)\frac{s_1}{c}\cos\beta_i\sin\alpha_j + F_y(s_1,s_2)\left(\sin\beta_i\sin\alpha_j + \frac{s_2}{c}\cos\beta_i\sin\alpha_j\right) \tag{2.16c}$$

in which x,y,z and x',y',z' are interrelated by Eq. 2.14 and Eq. 2.13 relates s_1, s_2, c to s_1', s_2', c'.

2.2.4. The Vectorial Angular Spectrum of the Receiving Antenna

The receiving antenna R in Fig. 1.2 is located at the origin of the x'y'z'-system with its aperture lying in x'y'-plane.

According to the reciprocity theorem, the transmitting and receiving characteristics of an antenna and identical. Therefore to determine the angular spectrum of antenna R it may be considered as a transmitting antenna. Then at a point P(x',y',z') in region $z' > 0$, the electric field will be given by a similar expression to that in Eq. 2.6. Denoting this field by $\bar{E}_R(x',y',z')$, one has the expression:

$$\bar{E}_R(x',y',z') = \int_{-\infty}^{\infty}\int_{-\infty}^{\infty}\Big[c'F^R_{x'}(s_1',s_2')\bar{e}_{x'}+c'F^R_{y'}(s_1',s_2')\bar{e}_{y'}-(s_1'F^R_{x'}(s_1',s_2') + s_2'F^R_{y'}(s_1',s_2'))\Big]\, e^{-jk\left[s_1'x'+s_2'y'+c'z'\right]}\frac{ds_1'ds_2'}{c'} \tag{2.17}$$

At large distances, i.e., at the radiation zone, the electric field may be represented in its asymptotic form as:

$$\bar{E}_R(\bar{r}')\Big|_{\text{far field}} = \bar{F}^R(s_1',s_2')\,\frac{e^{-jkr'}}{kr'} \tag{2.18}$$

where $\bar{F}^R(s_1',s_2')$ is the far-field radiation pattern of antenna R expressed as a function of direction cosines, which also corresponds to the vectorial angular spectrum function of R.

Therefore, in order to determine the vectorial angular spectrum $\bar{F}^R(s_1',s_2')$, the asymptotic form of $\bar{E}_R$ in Eq. 2.17 must be evaluated and this result must be compared with that in Eq. 2.18.

The method of stationary phase can be utilized to obtain the radiation field which is given by the first term of the evaluation as discussed in Appendix II. The result is:

$$\bar{E}_R(\bar{r}')\Big|_{\text{far field}} = 2\pi c' e^{j\frac{\pi}{2}} \frac{e^{-jkr'}}{kr'} \Big\{ F^R_{x'}(s_1', s_2')\bar{e}_{x'} + F^R_{y'}(s_1', s_2')\bar{e}_{y'}$$

$$- \frac{1}{c'}\left[s_1' F^R_{x'}(s_1', s_2') + s_2' F^R_{y'}(s_1', s_2') \right] \bar{e}_{z'} \qquad (2.19)$$

Hence in the right hand side of the above equation the vectorial angular spectrum of antenna R is the part except the term $\frac{e^{-jkr'}}{kr'}$. The transmitting antenna will, in general, have exactly the same form radiation field expressed w.r.t the (xyz)-system.

2.2.5. Received Signal in the Waveguide of the Receiving Antenna

By using Eqs. 2.8 and 2.19, the received signal, D, at a reference cross-section in the waveguide of antenna T, when illuminated by a plane wave given by Eqs. 2.15 and 2.16, can be expressed as,

$$D = K_1 \Big\{ c' b_{x'} F^R_{x'} + c' b_{y'} F^R_{y'} - b_{z'} \left[s_1' F^R_{x'} + s_2' F^R_{y'} \right] \Big\} e^{-jk[s_1 x + s_2 y + cz]}\Big|_{x'=y'=z'=0} \qquad (2.20a)$$

where $$K_1 = \frac{Y_o A \lambda}{k} \qquad (2.20b)$$

Therefore using Eqs. 2.13 and 2.14, after some laborious manipulations, one obtains

$$\exp\left\{ -jk\left[s_1 x + s_2 y + cz \right] \right\}\Big|_{x'=y'=z'=0} = \exp\left\{ -jk(s_1' \eta_m - s_2' \xi_n - c' \zeta_d) \right\} \qquad (2.21)$$

The signal received by the antenna R when antenna T is radiating, is obtained by integrating D in Eq. 2.20 over all possible directions of propagation. In other words, in the angular spectrum representation, the contribution of all plane waves that build up the resultant field have to be considered.

Thus using Eqs. 2.16a,b,c and Eq. 2.21 in Eq. 2.20, the resultant received signal, $D(\alpha_j, \beta_i, \varphi_m, \theta_n)$ can be expressed as

$$D_{ij}^{mn} = K_1 \iint_{-\infty}^{\infty}\left[F_{x'}^{R}F_{x}^{T}f_1+F_{x'}^{R}F_{y}^{T}f_2+F_{y'}^{R}F_{x}^{T}f_3+F_{y'}^{R}F_{y}^{T}f_4\right] e^{-jk\left[s_1'\eta_m-s_2'\xi_n-c'\zeta_d\right]} \frac{ds_1 ds_2}{c'} \quad (2.22)$$

where

$F_x^T = F_x^T(s_1,s_2)$ angular spectrum function of x-component of aperture electric field of T

$F_y^T = F_y^T(s_1,s_2)$ angular spectrum function of y-component of aperture electric field of T

$F_{x'}^R = F_{x'}^R(s_1',s_2')$ angular spectrum function of x'-component of aperture electric field of R

$F_{y'}^R = F_{y'}^R(s_1',s_2')$ angular spectrum function of y'-component of aperture electric field of R

$$f_1=f_1(s_1,s_2,s_1',s_2') = c'^2\sin\alpha_j - \frac{c'^2 s_1}{c}\cos\beta_i\cos\alpha_j - \frac{s_1 s_1' c'}{c}\cos\beta_i\sin\alpha_j \quad (2.23a)$$

$$f_2=f_2(s_1,s_2,s_1',s_2') = -c'^2\sin\beta_i\cos\alpha_j - \frac{c'^2 s_2}{c}\cos\beta_i\cos\alpha_j - \frac{c' s_1' s_2}{c}\cos\beta_i\sin\alpha_j - s_1' c'\sin\beta_i\sin\alpha_j \quad (2.23b)$$

$$f_3=f_3(s_1,s_2,s_1',s_2') = c'^2\cos\alpha_j + \frac{c'^2 s_1}{c}\sin\beta_i - \frac{s_2' s_1 c'}{c}\cos\beta_i\sin\alpha_j \quad (2.23c)$$

$$f_4=f_4(s_1,s_2,s_1',s_2') = -c'^2\cos\beta_i + \frac{c'^2 s_2}{c}\sin\beta_i - s_2' c'\sin\beta_i\sin\alpha_j - \frac{s_2' s_2 c'}{c}\cos\beta_i\sin\alpha_j \quad (2.23d)$$

and the relations between s_1, s_2, c and s_1', s_2', c' are given by Eq. 2.13.

Denoting the combination of the terms in brackets by $P(s_1, s_2, s_1', s_2')$, Eq. 2.22 takes on a simpler form given below

$$D_{ij}^{mn} = K_1 \int_{-\infty}^{\infty}\int_{-\infty}^{\infty} P(s_1, s_2, s_1', s_2')\, e^{-jk\left[s_1'\eta_m - s_2'\xi_n - c'\zeta_d\right]} \frac{ds_1 ds_2}{c'} \tag{2.24}$$

Eq. 2.22 gives both the amplitude and phase of the signal received by antenna R whose position is shown in Fig. 2.2

The formula in Eq. 2.22 is valid for any distance between the transmitting and the receiving antennas. Also the aperture distributions over the two antennas may have any polarization.

As the angular spectrum functions for the transmitting antenna is only defined for the wave propagating into the half-space $z > 0$, the multiple reflections between the two antennas are not taken into account. The neglection is valid provided that the seperation between the antennas is considerably larger than the maximum antenna dimensions and the wavelength, hence the effect of the multiple reflections may be ignored. Usually in the Fresnel region of the antenna, the effect of multiple reflections are negligible[KER 2].

The exponential term in Eq. 2.22 corresponds to the phase factor. It is a function of c. Hence for values of s_1 and s_2 that make c purely imaginary, an exponential decay factor is obtained which yields the contribution of the evanescent waves to the received signal. But it has been shown that the amplitude of the evanescent waves at a few wavelengths away from the transmitting aperture becomes negligible compared to the uniform plane waves[BIR 3]. Therefore in practical applications, the integration range in Eq. 2.22 may be restricted without much affecting the value of the integral.

2.3. Comparison of the Radiation Field with the Received Signal in the Far-Zone

In making direct far-field radiation pattern measurements the output of the measuring probe can be obtained by using Eq. 2.22. It should be noted that the asymptotic forms of Eqs. 2.6 and 2.7 which correspond to the far field expressions for the $\bar{E}$ and $\bar{H}$-fields respectively, do not represent the output of the measuring device.

The amplitude of the received signal, at the far field of the radiating structure is proportional to $\left[E_\theta^2+E_\varphi^2\right]^{1/2}$ in which E_θ and E_φ can be found from the asymptotic form of the $\bar{E}$-field. Hence to take the dot product of the unit vector denoting the polarization of the receiving probe with the far zone $\bar{E}$-field is not sufficient to describe the response of the measuring device to the radiated field.

In order to be more precise Eq. 2.22 need to be utilized directly because the asymptotic forms of the $\bar{E}$ and $\bar{H}$ fields hold exactly only at infinite distance. The transmission formula 2.22 which is valid at any distance, takes into account the directivity of the measuring probe as well, which can affect the received signal considerably specially in the sidelobe regions. Brown was the first one who demonstrated this point for the case in which the radiating antenna and the receiving probe are assumed to have uniform and Gaussian illuminations respectively[BR 2].

2.4. Error Correction in the Fourier Transform Method of Radiation Pattern Determination

One of the classical and well known techniques of determining far-field radiation patterns of aperture type antennas is the Fourier transform technique[RAM].

It is known that the Fourier transform of the aperture electric field distribution yields the far-field radiation pattern. But the probe utilized to measure the electric field mainly introduces two types of errors. (i) It distorts the original electric field configuration (ii) it does not measure the true electric field as it possesses a directivity pattern.

In this section a method for rigorously correcting the errors mentioned in (ii) is presented. The correction method for the two dimensional systems has been also proposed [BIR 1] . To suit the most general case, the general transmission formula derived in Section 2.2 will be used.

The measuring probe antenna travels over the aperture of the transmitting antenna T. At all positions the apertures of two antennas are parallel. For the present configuration $\alpha_j = 90^\circ$, ρ_d, β_i are always equal to zero. Hence the measured signal D, is a function of $x = \eta_m$ and $y = \xi_n$. Since

$$s_1 = s_1', \quad s_2 = -s_2', \quad c = -c'$$

Eq. 2.22 takes the following form

$$D(x,y) = K_1' \iint_{-\infty}^{\infty}\left[F_x^R, F_x^T f_1 + F_x^R, F_y^T f_2 + F_y^R, F_x^T f_3 + F_y^R, F_y^T f_4\right] e^{jk[xs_1 - ys_2]} \frac{ds_1 ds_2}{c} \tag{2.25}$$

where

$f_1 = f_1(s_1, s_2) = s_1^2 - c^2$

$f_2 = f_2(s_1, s_2) = s_1 s_2$

$f_3 = f_3(s_1, s_2) = s_1 s_2$

$f_4 = f_4(s_1, s_2) = (1 - s_1^2)$

The aperture measurements can be performed by using a linearly polarized probe. Two independent sets of measurements may be performed by the same probe, rotating it by 90° in xy-plane w.r.t. its orientation in the first set of measurements. In that way, two spectrum functions associated with the antenna T may be determined. In the first set, aperture electric field of receiving probe will be polarized in y-direction and in the second set in x-direction. Hence for the first set of measurements $F^{R}_{x'}$ will be equal to zero and in the second set $F^{R}_{y'}$ will be identically equal to zero. Denoting the functions giving the received signal, corresponding to independent positions of the measuring probe by $D_y(x,y)$ and $D_x(x,y)$, and in Eq. 2.25 replacing s_2 by $-s_2$, one obtains:

$$D_y(x,y) = K_1' \iint_{-\infty}^{\infty\infty} F^{R}_{y'}(s_1,s_2)\left[(s_1^2-c^2)F^{T}_{x}(s_1,s_2)+(1-s_1^2)F^{T}_{y}(s_1,s_2)\right] e^{jk[xs_1+ys_2]} \frac{ds_1 ds_2}{c} \quad (2.26a)$$

and

$$D_x(x,y) = -K_1' \iint_{-\infty}^{\infty\infty} s_1 s_2 F^{R}_{x'}(s_1,s_2)\left[F^{T}_{x}(s_1,s_2)+F^{T}_{y}(s_1,s_2)\right] e^{jk[xs_1+ys_2]} \frac{ds_1 ds_2}{c} \quad (2.26b)$$

in which $F^{R}_{x'}(s_1,s_2) = F^{R}_{y'}(s_2,s_1)$.

Now both sides of Eqs. 2.26a,b may be multiplied by $e^{-jk[s_a x+s_b y]}$ and integrated over $-\infty \leq x \leq \infty$, $-\infty \leq y \leq \infty$.

Then, after substituting s_2 for s_a and s_1 for s_b one can show that:

$$\frac{1}{c} F^{R}_{y'}(s_1,s_2)\left[(s_1^2-c^2)F^{T}_{x}(s_1,s_2)+(1-s_1^2)F^{T}_{y}(s_1,s_2)\right] = K_1 \int_{-\infty}^{\infty}\int_{-\infty}^{\infty} D_y(x\ ,y\ ) e^{-jk[s_1x+s_2y]} dxdy \qquad (2.27a)$$

and

$$-\frac{s_1 s_2}{c} F^{R}_{x'}(s_1,s_2)\left[F^{T}_{x}(s_1,s_2)+F^{T}_{y}(s_1,s_2)\right] = K_1 \int_{-\infty}^{\infty}\int_{-\infty}^{\infty} D_x(x\ ,y\ ) e^{-jk[s_1x+s_2y]} dxdy \qquad (2.27b)$$

in which K_1 is a new constant. The right hand sides of the Eqs. 2.27a,b correspond to the double Fourier transforms of the functions $D_y(x,y)$ and $D_x(x,y)$.

Defining $\mathcal{F}_{xy}$ to be the double Fourier transform operator, from Eqs. 2.27a,b the expressions for $F^{T}_{x}(s_1,s_2)$ and $F^{T}_{y}(s_1,s_2)$ can be obtained as follows:

$$F^{T}_{x}(s_1,s_2) = K\,\frac{c[1-s_1^2]}{2s_1^2-c^2-1}\left[\frac{\mathcal{F}_{xy}\{D_y(x_1y)\}}{[1-s_1^2]F^{R}_{y'}(s_1,s_2)} + \frac{\mathcal{F}_{xy}\{D_x(x,y)\}}{s_1s_2F^{R}_{x'}(s_1,s_2)}\right] \qquad (2.28a)$$

$$F^{T}_{y}(s_1,s_2) = K\,\frac{c[s_1^2-c^2]}{s_2^2-s_1^2}\left[\frac{\mathcal{F}_{xy}\{D_y(x,y)\}}{[s_1^2-c^2]F^{R}_{y'}(s_1,s_2)} + \frac{\mathcal{F}_{xy}\{D_x(x,y)\}}{s_1s_2F^{R}_{x'}(s_1,s_2)}\right] \qquad (2.28b)$$

where K is a constant. The above two equations give the corrected angular spectrums of the antenna T from which the vectorial radiation pattern can be easily obtained as discussed in Section 2.2.4.

Therefore in order to correct for the errors due to measuring probe directivity it suffices to divide the uncorrected patterns by the directivity patterns of the probes. Also the factors such as $[s_1^2-c^2]$ etc, need to be taken into account as given in the above equations.

Usually the probes utilized have patterns which deviate from isotropic characteristics for large angles. Hence as the above equations imply, the use of directive probes in the Fourier transform method of pattern determination may give rise to considerable errors specially in the sidelobe region of the radiation pattern of the measured antenna.

If the measurements were made on a transverse plane, at a certain distance, say $z = l$, away from the aperture of T, then the correction procedure would still be the same, and the Eqs. 2.28a,b giving the corrected spectrums would not be much different.

Sometimes, it is more convenient to carry out the measurements on that plane parallel to the aperture provided that the transverse field decays rapidly exterior to some finite region close to the measured antenna [KER 1]. In this case, the factor exp [-jkcl] in the integrand of Eq. 2.22 need to be considered also. Then to account for the seperation between the aperture and measurement planes the right hand side of Eqs. 2.26a,b should be multiplied by the inverse of exp [-jkcl].

III. DETERMINATION OF FAR-FIELD RADIATION-PATTERNS FROM NEAR FIELD MEASUREMENTS

3.1. Integral Equation Formulation and Antenna Synthesis

In Section 2.2 of Chapter II it is shown that the vectorial three dimensional far-field radiation pattern can be expressed in terms of two independent angular spectrum functions which were associated with the tangential components of the aperture electric field. Hence the determination of these two spectrum functions completely specifies the far zone fields. Furthermore through the use of Eqs. 2.6 and 2.7 the complete electromagnetic field at any point in region $z > 0$ can be determined.

In this chapter, it is shown that the two independent angular spectrum functions $F_x^T(s_1,s_2)$ and $F_y^T(s_1,s_2)$ can be obtained from the general transmission formula 2.22. Eq. 2.22 is a Fredholm type integral equation of the first kind which can be solved for F_x^T and F_y^T by expanding these functions into orthogonal series. Then the integral equation can be enforced at a discrete number of measurement values, D's. As the spectrum functions of the receiving antenna are present in the formulation, the directive properties of the measuring probe are taken into account also. Measurements can beperformed at any distance to the measured antenna. The only restriction is that the ratio of the maximum linear dimension of the measuring probe to the seperation distance should not be too large to distort the original field configuration.

As it is well known, the condition to measure directly, the far-field radiation pattern of a microwave antenna, is to illuminate its aperture by a plane wavefront. This can be accomplished either

by going to the far-zone of the antenna and utilizing a nearly isotropic probe, so that the wavefront is approximately plane, or by using an infinitely large probe so that it can produce a plane wave-front at any distance to the measured antenna. In the latter case, the probe, due to the antenna reciprocity theorem, can either be a transmitting antenna or a receiving one.

The infinitely large receiving antenna will have infinitely large gain and hence infinitely narrow beam-width. In other words, the pattern of that antenna will be in the form of a delta function. Thus in the transmission Eq. 2.22 the receiving antenna may be considered to be functioning as an infinitely narrow-band space filter for the angular spectrum of the measured antenna T shown in Fig. 2.2. Therefore, if an infinitely large receiving antenna is employed, there will be no need to solve the integral equation.

However, the use of such a big antenna is neither practical nor the interaction between the two antennas will be small. But the effect of a large antenna may be simulated by vectorially summing up the signals measured over a large portion of a plane surface as illustrated in Fig. 3.1. Then a peaked function corresponding to the pattern of the "synthesized antenna" can be introduced into the integrand of the transmission formula. The special case of infinitely large synthesized antenna, then corresponds to Martsafey's proposal for directly measuring far-field patterns [MART].

In practice, the synthesized antenna will be limited in size. Therefore, for the accurate determination of the spectrum functions, solution of the integral equation is necessary. However the synthesized pattern can serve the purpose of reducing the integration limits, hence reducing the computational work.

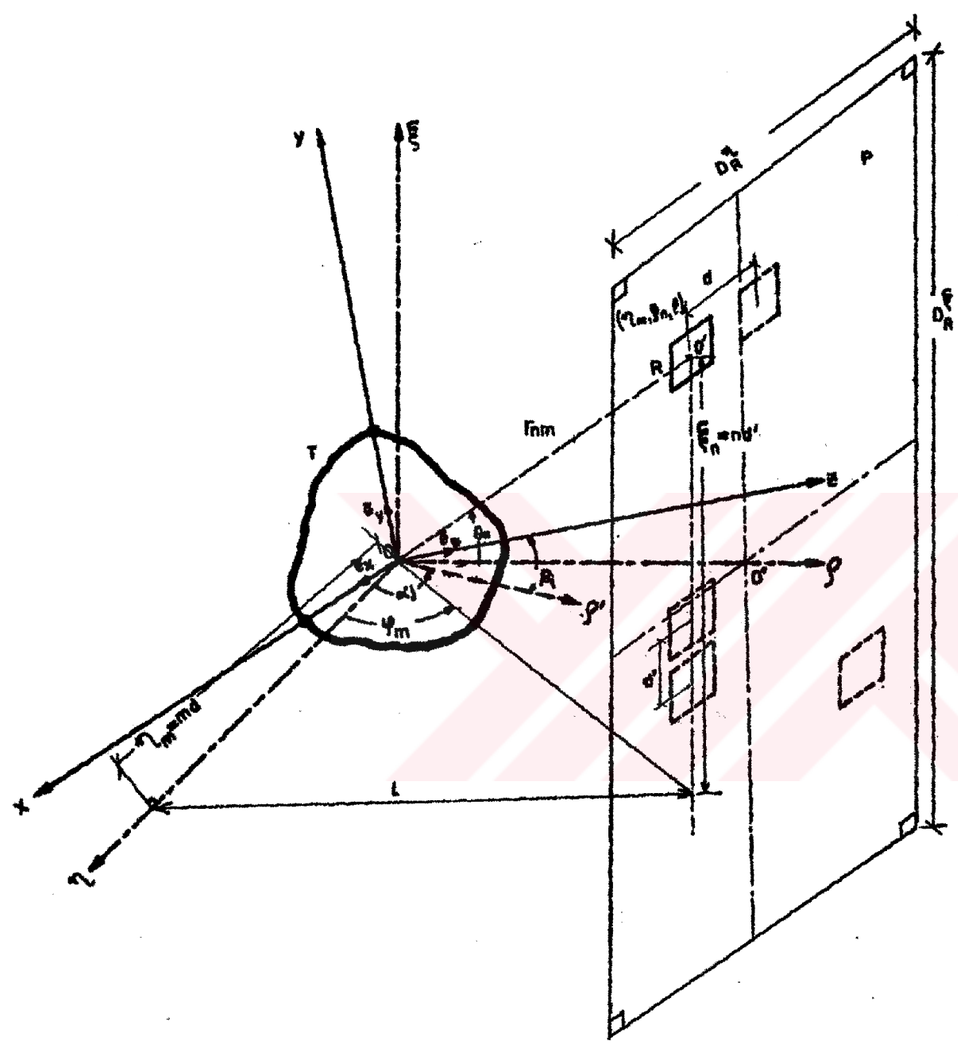

Fig. 3.1 Antenna Synthesis

One other advantage of the integral equation solution is the possibility of determination of the angular spectrum functions by means of which the far-zone vectorial fields can be expressed explicitly.

Now it will be shown that for a specific position of antenna T, by making phase and amplitude measurements over a plane surface $\rho = \ell$ (See Fig. 3.1) at suitable spacings to form a planar space array and summing these up vectorially, it is possible to produce the effect of a receiving antenna having a selective pattern. For this purpose the form of the transmission formula given by Eq. 2.24 will be utilized.

Consider that for a specific position of antenna T in Fig.3.1, specified by the angles (α_j, β_i), the probe R travels over the plane P such that it describes a (2M+1)(2N+1) measurement lattice.

Then with $\eta_m = md$, $\xi_n = nd'$ and $\rho_d = \ell$, the signal measured by R is given by:

$$D_{ij}^{mn} = K_1 \int_{-\infty}^{\infty}\int_{-\infty}^{\infty} p(s_1,s_2,s_1',s_2')\, e^{-jk[s_1'md-s_2'nd'-c'\ell]} \frac{ds_1 ds_2}{c'} \qquad (3.1)$$

Then by summing up the signals measured at all points in the lattice, the response of the synthesized antenna will be:

$$D_{ij} = \sum_{n=-N}^{N}\sum_{m=-M}^{M} D_{ij}^{mn} = K_1 \sum_n \sum_m \int_{-\infty}^{\infty}\int_{-\infty}^{\infty} p(s_1,s_2,s_1',s_2')$$

$$e^{-jk[s_1'md-s_2'nd'-c'\ell]} \frac{ds_1 ds_2}{c'} \qquad (3.2)$$

The order of the summation and the integration operations can be interchanged to yield

$$D_{ij} = K_1 \int_{-\infty}^{\infty}\int_{-\infty}^{\infty} p(s_1,s_2,s_1',s_2') e^{jk\ell c'} \left\{ \sum_{m=-M}^{M} e^{-jks_1'md} \sum_{n=-N}^{N} e^{jks_2'nd'} \right\} \frac{ds_1 ds_2}{c'} \tag{3.3}$$

Expressing the summation terms in closed form, one obtains:

$$D_{ij} = K_1 \int_{-\infty}^{\infty}\int_{-\infty}^{\infty} p(s_1,s_2,s_1',s_2') F^s(s_1',s_2') \; e^{+jk\ell c'} \; \frac{ds_1 ds_2}{c'} \tag{3.4}$$

where $F^s(s_1',s_2')$ denotes the angular spectrum function of the synthesized antenna which is given by:

$$F(s_1',s_2') = \frac{\mathrm{Sin}\left[kR_R^{\eta} s_1'\right]}{\mathrm{Sin}\left[\frac{ks_1'd}{2}\right]} \; \frac{\mathrm{Sin}\left[kR_R^{\xi} s_2'\right]}{\mathrm{Sin}\left[\frac{ks_2'd'}{2}\right]} \tag{3.5}$$

where

$$R_R^{\eta} = \frac{D_R^{\eta}}{2} = (2M+1)d/2 \tag{3.6a}$$

$$R_R^{\xi} = \frac{D_R^{\xi}}{2} = (2N+1)d'/2 \tag{3.6b}$$

Therefore, the effect of the antenna synthesis is to insert the function $F^s(s_1',s_2')$ into the integrand of Eq. 3.1. Larger M and N, i.e., larger the synthesized antenna, larger is the filtering effect.

3.2. Integral Equation Solution to Determine Far-Field Radiation-Pattern

The integral equation involving the unknown spectrums and the pattern of the synthesized antenna is given by:

$$D_{ij} = K_1 \iint_{-\infty}^{\infty} F^s(s_1', s_2') \left\{ F_x^T \left[F_{x'}^R f_1 + F_{y'}^R f_3 \right] + F_y^T \left[F_{x'}^R f_2 + F_{y'}^R f_4 \right] \right\} e^{jk\ell c'} \frac{ds_1 ds_2}{c'} \tag{3.7}$$

The solution to the above integral equation can be obtained by expanding the unknown functions in orthogonal series and thus converting the solution of the integral equation to a solution of a set of linear algebraic equations.

In Section 1 of Chapter II it was emphasized that far-field radiation patterns could be defined only for localized source distributions. Therefore the aperture field distributions of antennas for which a far-zone exits, are confined to a finite area in space. It is also shown that the antenna patterns and aperture electric field distributions are Fourier transform pairs. Thus, the angular spectrum function whose Fourier transform is the aperture electric field distribution which is limited in space, can be expanded into a sampling series by using Shannon's sampling theorem [PAP].

The sampling expansions for the angular spectrum functions $F_x^T(s_1, s_2)$ and $F_y^T(s_1, s_2)$ as given in Appendix 3 are;

$$F_x^T(s_1, s_2) = \sum_{m=-M}^{M} \sum_{n=-N}^{N} c_{nm}^x \, h_m(s_1) g_n(s_2) \tag{3.8a}$$

$$F_y^T(s_1, s_2) = \sum_{m=-M}^{M} \sum_{n=-N}^{N} c_{nm}^Y \, h_m(s_1) g_n(s_2) \tag{3.8b}$$

where

c_{nm}^x's and c_{nm}^y's are complex coefficients to be determined and $h_m(s_1)$ and $h_n(s_2)$ correspond to the "composing function" which are given by:

$$h_m(s_1) = \frac{\text{Sin } kR_x^T(s_1-mP_1)}{kR_x^T\ (s_1-mP_1)} \tag{3.9a}$$

$$g_n(s_2) = \frac{\text{Sin } kR_y^T(s_2-nP_2)}{kR_y^T(s_2-nP_2)} \tag{3.9b}$$

in which R_x^T and R_y^T correspond to the sides of a rectangle which is assumed to completely cover the aperture of antenna T. (Fig. 3.2a) P_1 and P_2 refer to the "periods" in the sampling expansions and are given by:

$$P_1 = \frac{\pi}{kR_x^T} \tag{3.10a}$$

$$P_2 = \frac{\pi}{kR_y^T} \tag{3.10b}$$

If the rectangle determined by R_x^T and R_y^T just covers the aperture of T, then the number of terms in the sampling expansion will be minimum corresponding to the Nyquist rate of sampling.

By selecting larger rectangles, higher sampling rates may be utilized and hence more terms can be obtained in the expansion.

On the other hand, if a circle with radius R_c is drawn to cover the aperture of T as in Fig. 3.2b, the form of the sampling expansions for $F_x^T(s_1,s_2)$ and $F_y^T(s_1,s_2)$ will then be given by (Appendix III)

$$F_x^T(s_1,s_2) = \sum_{n=-N}^{N}\sum_{m=-M}^{M} b_{nm}^x \frac{J_1\left\{\sqrt{(kR_c)^2\left[(s_1-mP)^2+(s_2-np)^2\right]}\right\}}{\sqrt{(kR_c)^2\left[(s_1-mP)^2+(s_2-nP)^2\right]}} \tag{3.11a}$$

$$F_y^T(s_1,s_2) = \sum_{n=-N}^{N}\sum_{m=-M}^{M} b_{mn}^y \frac{J_1\left\{\sqrt{(kR_c)^2\left[(s_1-mP)^2+(s_2-nP)^2\right]}\right\}}{\sqrt{(kR_c)^2\left[(s_1-mP)^2+(s_2-nP)^2\right]}} \tag{3.11b}$$

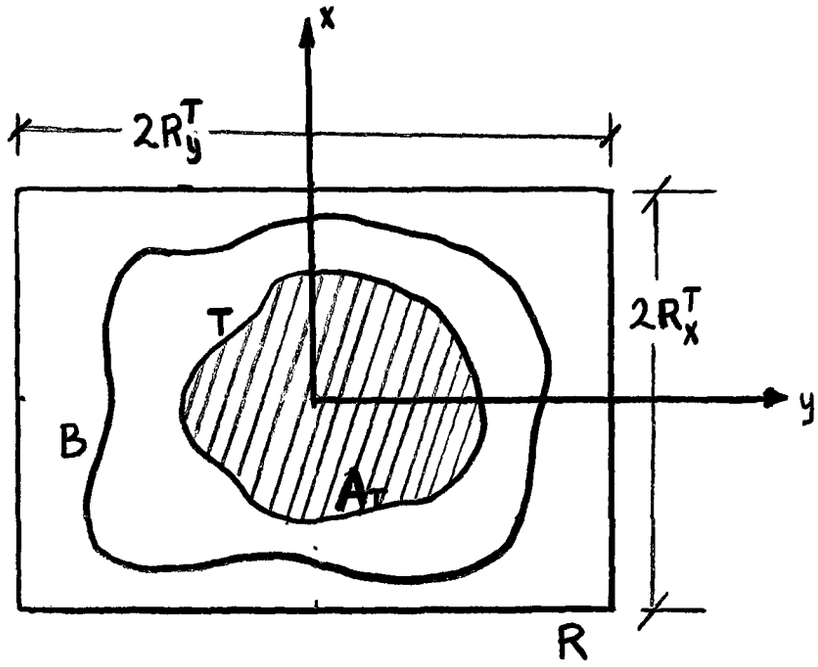

Fig. 3.2a Regions Governing the Expansion in Eq. 3.8

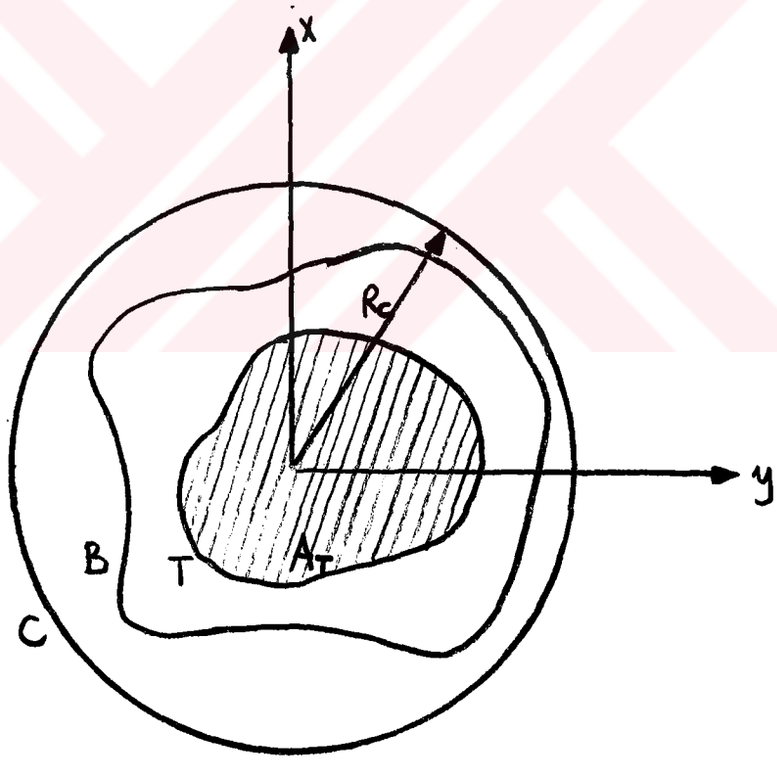

Fig. 3.2b Regions Governing the Expansion in Eq. 3.11

where

$$P = \frac{\pi}{kR_c} \tag{3.12}$$

and $J_1\{\ldots\}$ is the first order Bessel function of the first kind.

Due to the measurement limitations, all the sampling expansions are truncated. The minimum number of terms in the sampling expansions is determined by the maximum optical size, kD_{max}, of antenna T. This minimum number is equal to MM where MM is the integer just greater than the ratio $(2\frac{D_{max}}{\lambda} + 1)$ where D_{max} is the maximum linear dimension of T and λ is the wavelength. (MM is defined over one of the summations.)

Two independent sets of measurements can be performed for two independent orientations of probe R. If in the second set of measurements, R is rotated by 90° around z'-axis, w.r.t its orientation in the first set of measurements, then:

$$F^R_{x'} \rightarrow F^R_{y'} \quad \text{and} \quad F^R_{y'} \rightarrow F^R_{x'}$$

Hence substituting the expansions given by equations (3.8a,b) into the integral Eq. 3.7 and interchanging the orders of integration and summation operations, one obtains:

$$D''_{ij} = \sum_n \sum_m I''_{ijnm}\, c^x_{nm} + \sum_n \sum_m II''_{ijnm}\, c^y_{nm} \tag{3.13a}$$

$$D^{\perp}_{ij} = \sum_n \sum_m I^{\perp}_{ijnm}\, c^x_{nm} + \sum_n \sum_m II^{\perp}_{ijnm}\, c^y_{nm} \tag{3.13b}$$

where

D''_{ij}: refers to the received signal by the synthesized antenna when R is oriented such that y'-axis of receiving system is parallel to the ξ-axis of fixed coordinate system.

$D_{ij}^{\perp}$: refers to the received signal by the synthesized antenna when R is oriented such that the y'-axis of receiving system is perpendicular to the ξ -axis of the fixed coordinate systems.

and

$$I''_{ijnm} = K_1 \int_{-\infty}^{\infty}\int_{-\infty}^{\infty} F^s(s_1',s_2')\left[F_{x'}^R f_1 + F_{y'}^R f_3\right] h_m(s_1) g_n(s_2) e^{jk\ell c'} \frac{ds_1 ds_2}{c'} \tag{3.14a}$$

$$II''_{ijnm} = K_1 \int_{-\infty}^{\infty}\int_{-\infty}^{\infty} F^s(s_1',s_2')\left[F_{x'}^R f_2 + F_{y'}^R f_4\right] h_m(s_1) g_n(s_2) e^{jk\ell c'} \frac{ds_1 ds_2}{c'} \tag{3.14b}$$

$$I_{ijnm}^{\perp} = K_1 \int_{-\infty}^{\infty}\int_{-\infty}^{\infty} F^s(s_1',s_2')\left[F_{y'}^R f_1 + F_{x'}^R f_3\right] h_m(s_1) g_n(s_2) e^{jk\ell c'} \frac{ds_1 ds_2}{c'} \tag{3.14c}$$

$$I_{ijnm}^{\perp} = K_1 \int_{-\infty}^{\infty}\int_{-\infty}^{\infty} F^s(s_1',s_2')\left[F_{y'}^R f_2 + F_{x'}^R f_4\right] h_m(s_1) g_n(s_2) e^{jk\ell c'} \frac{ds_1 ds_2}{c'} \tag{3.14d}$$

It should be noted that by using a linearly polarized probe it is possible to perform two independent sets of measurements and simplify the equations given by Eqs. 3.14a,b,c,d further. Then in the first set of measurements $F_{x'}^R \neq 0$, $F_{y'}^R = 0$ and in the second set $F_{y'}^R \neq 0$, $F_{x'}^R = 0$.

Thus enforcing the integral equation at a discrete number of measurement values, one obtains Eqs. 3.13a,b which can be solved for the unknown coefficients.

The integrals in Eqs. 3.14a, b, c, d which consist of known functions can be evaluated by using a digital computer. The integration over s_1 and s_2 exterior to the unit circle determined by $s_1^2+s_2^2+c^2 = 1$ may be neglected since it corresponds to the contribution of the evanescent waves to the received signal which is very small[BIR 3]. The filtering effect of the synthesized pattern $F^s(s_1,s_2)$ enables a further reduction of the integration limits. The phase factor, $\exp[jk\ell c']$ has also additional filtering effect.

Since $-N \leq n \leq N$ and $-M \leq m \leq M$, to determine the three dimensional radiation pattern of antenna T, 2(2N+1)(2M+1) independent measurement values are necessary. As pointed out earlier the minimum of the limits M and N depend upon the size of the rectangle in Fig. 3.2 which is just larger than the maximum optical dimensions of the antenna.

Equations 3.13a,b can be put into a matrix form to read:

$$[D''] = [I''][c^x] + [II''][c^y] \tag{3.15a}$$

$$[D^{\perp}] = [I^{\perp}][c^x] + [II^{\perp}][c^y] \tag{3.15b}$$

or combining these we have

$$\begin{bmatrix} [D''] \\ \hline [D^{\perp}] \end{bmatrix} = \left[\begin{array}{c|c} [I''] & [II''] \\ \hline [I^{\perp}] & [II^{\perp}] \end{array}\right] \begin{bmatrix} [c^x] \\ \hline [c^y] \end{bmatrix} \tag{3.16}$$

Further with a simpler notation,

$$[D] = [I][c] \tag{3.17}$$

where

$[D]$ is the 2(2N+1)(2M+1)x1 "measurement matrix"

$[I]$ is the 2(2N+1)(2M+1)x2(2N+1)(2M+1) "integral matrix"

$[C]$ is the 2(2N+1)(2M+1)x1 "coefficient matrix"

It can be shown that $[I]^{-1}$ exists and from Eq. 3.17 we obtain

$$[C] = [I]^{-1} [D] \tag{3.18}$$

Thus, once the coefficients $[C]$ are obtained from the above equation, they can be used in Eqs. 3.8a,b to determine the angular spectrum functions. Then the three dimensional vectorial far-field radiation pattern of antenna T can be expressed by using the spectrum functions.

The angles (α_j, β_i) specifying the orientation of antenna T can be selected such that the peaks of the composing functions coincide with the peak of the synthesized pattern thus making the diagonal entries of the integral matrix larger than the other entries of the corresponding row.

It is also possible to obtain the angular spectrum functions from integral equation solution without synthesizing an antenna. Then in integrals 3.14a,b,c,d the pattern of the synthesized antenna should be taken to be equal to unity. But in that case no filtering effect will be present and thus the computational work will increase. Furthermore, the antenna synthesis technique, reduces the error in values of the pattern near the x-axis, due to the truncation of the sampling series. This error is maximum near the limits of integration and decreases near zero angle values. The synthesized pattern, as it reduces the integration limits, for near-axis α_j and β_i values, causes the effect of this error to be less.

It should be noted that an integral matrix which is computed for an antenna of given optical size can be utilized for antennas of smaller optical dimensions.

3.3. The Limiting Case of an Infinitely Large Synthesized Antenna

The integral given by Eq. 3.7 can be expressed w.r.t the variables s_1', s_2', in the following form

$$D_{ij} = K_1 \int_{-\infty}^{\infty}\int_{-\infty}^{\infty} F^s(s_1',s_2') \left\{ F_x^T \left[F_{x'}^R f_1 + F_{y'}^R f_3\right] + F_y^T \left[F_{x'}^R f_2 + F_{y'}^R f_4\right] \right\} \left|J(s_1',s_2')\right| e^{jk\ell_{c'}} \frac{ds_1' ds_2'}{c'} \tag{3.19}$$

where $J(s_1',s_2')$ is the Jacobian determinant of the transformation between s_1, s_2 and s_1', s_2' whose expression is given by;

$$J(s_1',s_2') = \begin{vmatrix} \dfrac{\partial s_1}{\partial s_1'} & \dfrac{\partial s_2}{\partial s_1'} \\ \dfrac{\partial s_1}{\partial s_2'} & \dfrac{\partial s_2}{\partial s_2'} \end{vmatrix} = \operatorname{Cos}\beta_i \left(\frac{s_1'}{c'} \operatorname{Cos}\alpha_j - \operatorname{Sin}\alpha_j \right) - \frac{s_2'}{c'} \operatorname{Sin}\beta_i \operatorname{Cos}2\alpha_j \tag{3.20}$$

From Eq. 3.5, $F^s(s_1',s_2')$ can be written in the form:

$$F^s(s_1',s_2') = F_1(s_1')F_2(s_2') = \frac{\operatorname{Sin}\left[kR_R^{\eta} s_1'\right]}{kR_R^{\eta} s_1'} \cdot \frac{kR_R^{\eta} s_1'}{\operatorname{Sin}\left[\frac{ks_1'd}{2}\right]} \cdot \frac{\operatorname{Sin}\left[kR_R^{\xi} s_2'\right]}{kR_R^{\xi} s_2'} \cdot \frac{kR_R^{\xi} s_2'}{\operatorname{Sin}\left[\frac{ks_1'd}{2}\right]} \tag{3.21}$$

For the case of an infinitely large synthesized antenna, Eq. 3.19 takes on the form

$$D_{ij} = K_1 \lim_{\substack{R_R^{\eta}\to\infty \\ R_R^{\xi}\to\infty}} \iint_{-\infty}^{\infty} F_1(s_1')F_2(s_2')\left\{ F_x^T\left[F_x^R, f_1 + F_y^R, f_3\right] + F_y^T\left[F_x^R, f_2 + F_y^R, f_4\right]\right\} \left|J(s_1', s_2')\right| e^{jk\ell c'} \frac{ds_1' ds_2'}{c'} \qquad (3.22)$$

$$D_{ij} = K_3\, e^{jk\ell}\left\{ F_x^T(\alpha_j, \beta_i)\left[F_x^R, f_1 + F_y^R, f_3\right]\Big|_{s_1'=s_2'=0} + F_y^T(\alpha_j, \beta_i) \cdot \left[F_x^R, f_2 + F_y^R, f_4\right]\Big|_{s_1'=s_2'=0}\right\} \left|J(0,0)\right| \qquad (3.23)$$

where K_3 is a new constant.

One can therefore observe the fact that when an infinitely large antenna is synthesized, the response of the synthesized antenna will be given by the expression in Eq. 3.23 which is not directly equal to the far field radiation pattern. This contrasts Martsafey's argument that by synthesyzing a very large antenna, it is possible to measure far-field pattern directly.

Note again that making two independent sets of measurements corresponding to two independent orientations of the probe R, $F_x^T(\alpha_j, \beta_i)$ and $F_y^T(\alpha_j, \beta_i)$ can be obtained. Consequently the vectorial three dimensional radiation pattern can be expressed in terms of them.

In this limiting case, the synthesized pattern may be considered to be functioning as an angular filter with infinitely high resolution.

IV. APPLICATION TO FANNED-BEAM ANTENNAS

In this chapter the determination of far-field radiation-patterns of fanned beam microwave antennas with linearly polarized aperture electric field distributions are considered.

Some examples of antennas having fan shaped beams are: sectoral horns, symmetrically cut paraboloids, parabolic cylinder antennas, cheese and pillbox antennas [SIL].

In order to determine the radiation-patterns from near-field measurements, the theory developed in Chapter III is utilized. Antenna synthesis is achieved by moving the receiving probe in the principal plane containing the narrow-beam of the three dimensional radiation pattern.

4.1. Transmission Formula for Fanned-Beam Antennas Having Linearly Polarized Aperture Electric Field Distributions

For the determination of H-plane far-field radiation-patterns of fanned-beam antennas, consider antenna T, and the receiving probe R, shown in Fig. 4.1. It is assumed that both of these antennas have their aperture electric fields polarized in η-direction. The angular spectrum functions $F_y^T(s_1,s_2)$ and $F_{y'}^R(s_1',s_2')$, which are respectively associated with the y- and y'-components of the aperture electric fields of antennas T and R are, equal to zero.

Hence Eq. 2.22 takes the form:

$$D_{ij} = K_1 \int_{-\infty}^{\infty}\int_{-\infty}^{\infty} f_1(s_1,s_2,s_1',s_2') F_{x'}^R(s_1',s_2') F_x^T(s_1,s_2)\, e^{-jk\ell c'} \frac{ds_1 ds_2}{c'} \tag{4.1}$$

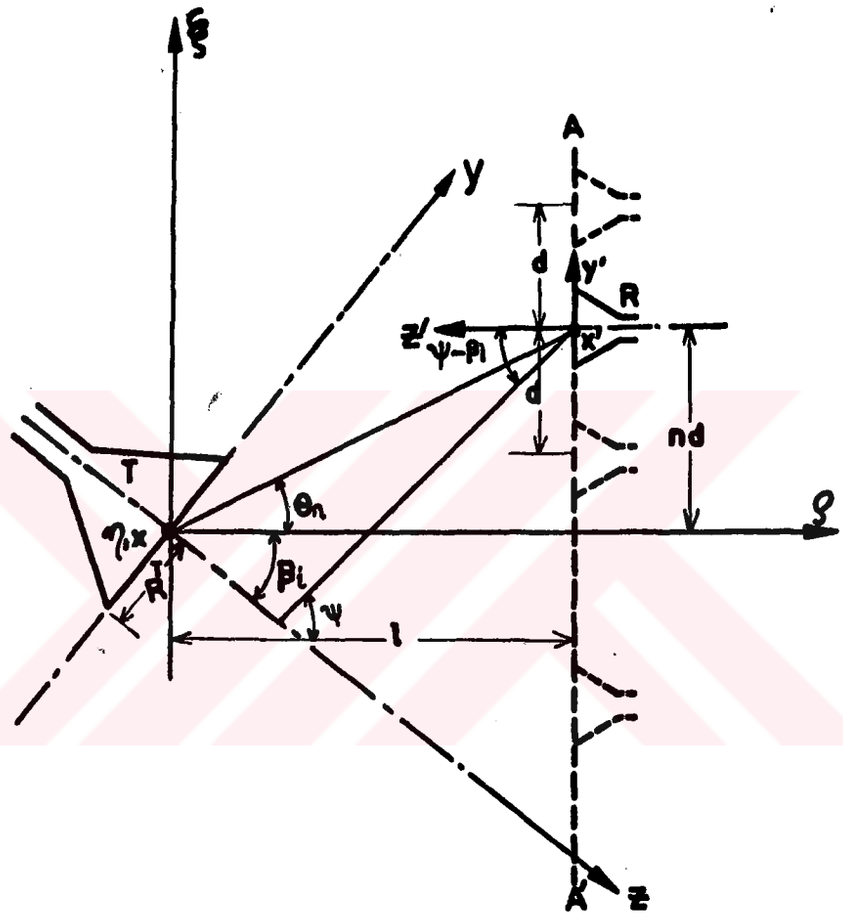

Fig.4.1 Near-Field Measurements on $\xi\rho$ -plane

As it is well known, the most common way of producing fanned beams is to make the aperture dimensions in the two principal planes highly different [SIL] . In the present case, antennas having much larger aperture dimensions in the H-plane than the dimensions in the E-plane are considered. Then the antennas T and R shown in Fig. 2.2 and Fig. 4.1 have much narrower beamwidths in H-plane than their beamwidths in E-plane. That is to say, $F_x^T(s_1,s_2)$ and $F_{x'}^R(s_1',s_2')$ varies much more rapidly with s_2 than they do with s_1. Since the antenna synthesis was performed in the H-plane with $\alpha_j = \varphi_m = 90^o$ (Fig. 2.2 and Fig. 4.1), the synthesized antenna has a much narrower beam in H-plane then its beam in E-plane. Under these conditions the integrand in Eq. 4.1 excluding the exponential term, varies much more slowly with s_1 compared to the rate of variation w.r.t s_2. Hence, provided that ℓ, the seperation between the measured and synthesized antennas is greater than some minimum value (which can be taken as the Rayleigh distance for the smaller aperture dimension), the integral with respect to s_1 can be evaluated by the method of stationary phase to yield; (Appendix 4)

$$D(\beta_i) = \frac{K}{\sqrt{\cos\beta_i}} \int_\Gamma (1-s_2^2)^{\frac{1}{4}} F^s(s_2') F_x^T(s_2) F_{x'}^R(s_2') \, e^{-jk\ell[\cos\beta_i c - \sin\beta_i s_2]} (1-s_2'^2) ds_2 \qquad (4.2)$$

where $F^s(s_2')$ is the H-plane pattern of the synthesized antenna which is given by:

$$F^s(s_2') = \frac{\sin\left[kR^s s_2'\right]}{\sin\left[\frac{kd}{2} s_2'\right]} \qquad (4.3)$$

with $s_2 = \sin\psi$, Eq. 4.2 becomes:

$$D(\beta_i) = \frac{K}{\sqrt{\cos\beta_i}} \int_\Gamma \cos^{\frac{3}{2}}\psi \, \cos(\psi+\beta_i) F^s[\sin(\psi+\beta_i)] \, F_x^T[\sin\psi] \, F_{x'}^R[\sin(\psi+\beta_i)] \, e^{-jk\ell\cos(\psi+\beta_i)} d\psi \qquad (4.4)$$

where the integration contour Γ, is as illustrated in Fig. 4.2a.

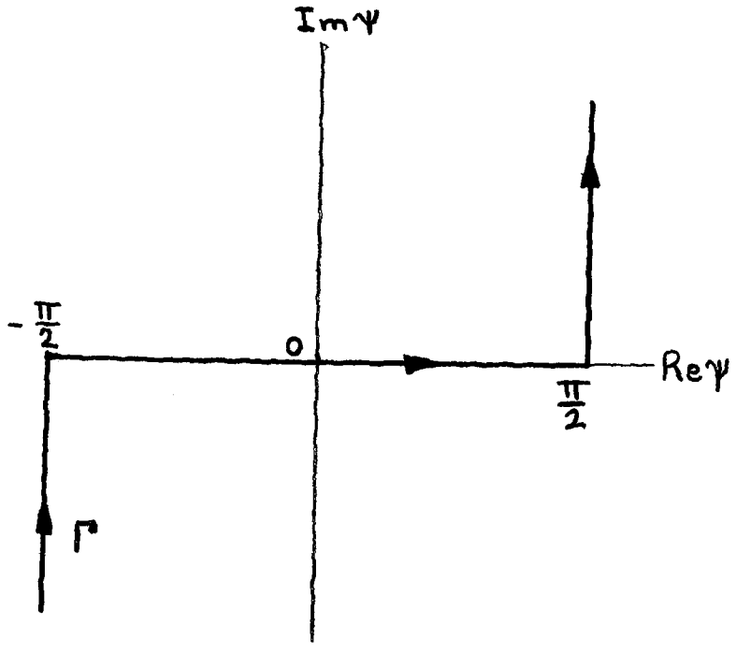

Fig. 4.2a Integration Contour for Eq. 4.4

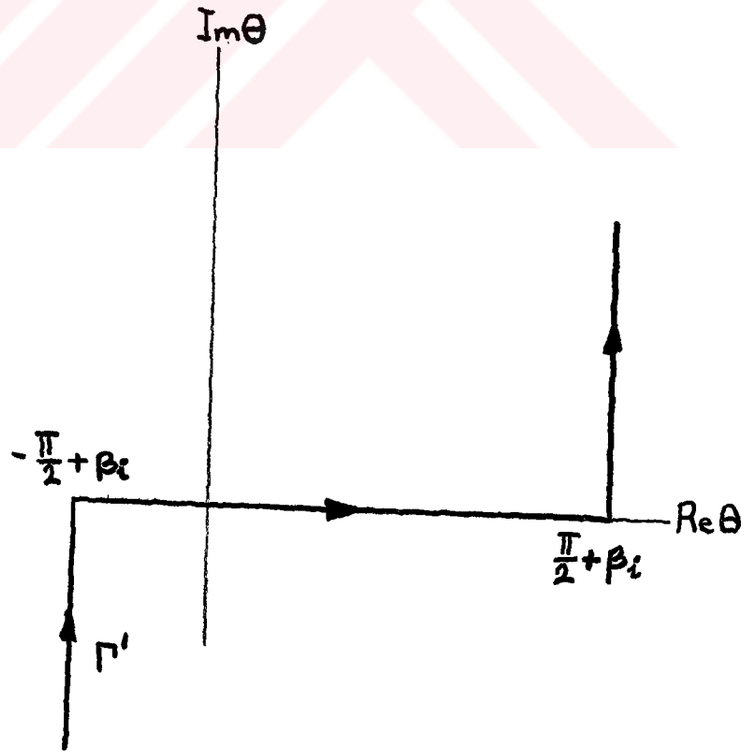

Fig. 4.2b Integration Contour for Eq. 4.14

The integration over the complex angles represents the contribution of the evanescent waves to the received signal. At a few wavelengths away from the source, this contribution is negligible [BOO]. Therefore the integration will be restricted to real angles only.

4.2. Determination of the Radiation Pattern by Integral Equation Solution

The angular spectrum function $F_x^T[\mathrm{Sin}\psi]$ can be determined from the solution of the integral Eq. 4.4 in which $D(\beta_i)$ represents the response of the synthesized antenna.

To solve the integral equation, the unknown, $F_x^T(s_2)$, whose inverse Fourier transform is "space limited" will be expanded into a sampling series; (Appendix 3) with $s_2 = \mathrm{Sin}\,\psi$,

$$F_x^T[\mathrm{Sin}\psi] = \sum_{n=-N}^{N} c_n g_n[\mathrm{Sin}\psi] \tag{4.5}$$

where

$$g_n[\mathrm{Sin}\psi] = \frac{\mathrm{Sin}\,kR^T[\mathrm{Sin}\psi - nP]}{kR^T[\mathrm{Sin}\psi - nP]} \tag{4.6}$$

with

$$P = \frac{\pi}{kR^T} \tag{4.7}$$

The minimum number of terms in the expansion is determined by the largest optical size.

In general one must have $R^T \geqslant R_y^T$, where the equality sign of T holds for the sampling expansion containing the minimum number of terms.

Using the expansion 4.5, Eq. 4.4 takes the form:

$$D(\beta_i) = \sum_{n=-N}^{N} c_n I_{in} \tag{4.8}$$

In this summation the minimum number of terms, N, that must be considered is given by $(2N_{min}+1)$ where N_{min} is the least integer greater than the ratio $\frac{2R_y^T}{\lambda}$. R_y^T stands for the largest linear dimension of antenna T in y-direction measured from O. (Fig.4.1) The terms, I_{in}'s in Eq. 4.8 are given by:

$$I_{in} = \frac{K}{\sqrt{\cos\beta_i}} \int_{-\frac{\pi}{2}+\Delta\theta_o}^{\frac{\pi}{2}+\Delta\theta_o} \cos^{\frac{3}{2}}\psi \cos(\psi+\beta_i) F^s[\sin(\psi+\beta_i)]$$

$$g_n[\sin\psi] F_{x'}^R[\sin(\psi+\beta_i)] e^{-jk\ell\cos(\psi+\beta_i)} d\psi \tag{4.9}$$

In this last equation, the limits of integration are purposely reduced due to the combined filtering effect of the synthesized pattern and the exponential factor.

Now Eq. 4.8 can be expressed in matrix form as

$$[D] = [I][C] \tag{4.10}$$

where

$[D]$ is the "measurement" vector of order (2N+1):

$$[D] = \begin{bmatrix} D(\beta_{-N}) \\ \vdots \\ D(\beta_o) \\ D(\beta_1) \\ \vdots \\ D(\quad_N) \end{bmatrix} \tag{4.11}$$

$[I]$ is the (2N+1)x(2N+1) "integral" matrix:

$$[I] = \begin{bmatrix} I_{-N,-N} & I_{-N,-N+1} & \cdots & \\ \vdots & & & \\ I_{0,-N} & I_{0,0} & & \\ \vdots & & \ddots & I_{i,n} \\ & & & \vdots \\ I_{N,-N} & \cdots & & I_{NN} \end{bmatrix} \tag{4.12}$$

And $[C]$ is the "coefficient" vector of order 2N+1:

$$C = \begin{bmatrix} C_{-N} \\ \vdots \\ C_{o} \\ \vdots \\ C_{N} \end{bmatrix} \tag{4.13}$$

To obtain the entries of $[D]$, for each specific angular position, β_i, of antenna T, the signals received by the probe R in distinct positions are added vectorially.

The measurement angles, β_i's, can be selected such that the maximums of the composing functions $g_n[\mathrm{Sin}\,\psi]$ coincide with the peak of the synthesized pattern. Therefore, since the stationary point occurs also at $\psi = -\beta_i$, the diagonal elements of the matrix $[I]$ can be made considerably larger than the off-diagonal elements if the filtering effect in sufficiently large. This procedure enables the simplification of the matrix $[I]$, by taking the comparitevely negligible entries as zero. This point is verified in Section 4.3 concerned with numerical investigations.

In Eq. 4.9 using the transformation $\theta = \psi + \beta_i$, one obtains:

$$I_{in} = \frac{K}{\sqrt{\mathrm{Cos}\,\beta_i}} \int_{-\Delta\theta_o}^{\Delta\theta_o} \mathrm{Cos}^{\frac{3}{2}}(\theta-\beta_i)\,\mathrm{Cos}\,\theta\; F^s[\mathrm{Sin}\,\theta]\, F^R_{x'}[\mathrm{Sin}\,\theta]\; g_n[\mathrm{Sin}(\theta-\beta_i)]\; e^{-jk\ell\,\mathrm{Cos}\,\theta}\, d\theta \tag{4.14}$$

where

$$g_n\left[\operatorname{Sin}(\theta-\beta_i)\right] = \frac{\operatorname{Sin} kR^T\left[\operatorname{Sin}(\theta-\beta_i)-nP\right]}{kR^T\left[\operatorname{Sin}(\theta-\beta_i)-nP\right]} \tag{4.15}$$

The measurement angles may be fixed according to the relation:

$$\beta_i = \operatorname{Sin}^{-1}(iP) \tag{4.16}$$

Thus, the use of the sampling expansion of the unknown pattern in the integral equation solution has the following advantages:

(i) It enables the use of minimum number of terms to represent the unknown.

(ii) By fixing the measurement angles according to the relation given by Eq. 4.16, the integral matrix can be simplified by setting some of the off-diagonal elements to zero. This can faciliate the inversion of some large integral matrices.

(iii) As the composing functions in the expansion are of decaying nature, the effect of the truncation error on the spectrum of antenna T is decreased considerably around the near zero-degree angles. This property is largely assisted by the restriction of integration range due to the combined filtering action of the phase factor and the synthesized pattern.

The antenna synthesis technique, besides reducing the computational work, can thus provide means for accurate representation of the angular spectrum of antenna T, near the zero-degree angles.

From Eq. 4.10, the coefficient matrix can be obtained as:

$$[C] = [I]^{-1}\,[D] \tag{4.17}$$

Then once the coefficients of the sampling expansion are determined from Eq. 4.17, they can be used in Eq. 4.5 to determine $F_x^T[\mathrm{Sin}\,\psi]$.

The entries of the integral matrix can be determined from Eq. 4.14 by using the digital computer. (Appendix V). It should be noted that $[I]$ is not dependent upon the measurement values and the integral matrix computed for an antenna of certain optical-size can be used for antennas of smaller optical sizes as well. This point is also demonstrated in Chapter V concerned with the experimental results.

With $\alpha_j = \frac{\pi}{2}$, Eq. 4.1 can be approximated by the first term of the stationary phase evaluation [PAP] to obtain the response of a probe located at the far-field of antenna T.

The result is:

$$D(\beta_i) = K_1'' \mathrm{Cos}\,\beta_i F_x^T[0,\beta_i]\, F_{x'}^R[0,0]\, F^s[0,0]\frac{e^{-jkr}}{kr} \qquad (4.18)$$

where K_1'' is a constant.

The power received by R is then:

$$\left|D(\beta_i)\right|^2 = \frac{\left|K_1''\right|^2}{[kr]^2}\mathrm{Cos}^2\beta_i \left|F_x^T(0,\beta_i)\right|^2 \left|F_{x'}^R[0,0]\right|^2 \left|F^s(0,0)\right|^2 \qquad (4.19)$$

Therefore the far-field power pattern of antenna T can be obtained by multiplying $\left|F_x^T[\mathrm{Sin}\,\psi]\right|^2$ by $\mathrm{Cos}^2\psi$.

4.3. Numerical Investigations

This section deals with the computerized check-up of the method of integral equation solution to determine the far-field radiation patterns. For this purpose, first the angular spectrum

function, $F_x^T[\sin\psi]$, of antenna T is taken to be a known function, such as the one resulting from a uniform, cosine, cosine with linear phase variation or cosine squared aperture electric field distribution.

Then using the transmission formula given by Eq. 4.4, the signals which would yield the response of the synthesized antenna in the near-field of antenna T are computed by using the digital computer. Afterwards these near field signals are fed into the computer as input data specifying the "measurement" matrix. The entries of the integral matrix are evaluated by using the Gaussian quadrature method of numerical integration [FRO]. Integral matrix is then inverted and the coefficients of the sampling expansion are determined by using Eq. 4.16. Eq. 4.5 is then utilized to determine the angular spectrum function $F_x^T[\sin\psi]$ which can be compared with the assumed spectrum function.

Extreme care should be taken in the numerical evaluation of the entries of the integral matrix which may consist of integrals with rapidly varying integrands[BIR 3].

The effect of various size synthesized antennas in reducing the computational work can be studied by means of this computer simulation. However it should be noted that this simulation checks the principle involved in far-field pattern determinations but not the validity of the experimental model associated with the mathematical formulation.

In this thesis various errors that may be introduced in the application of the method to fanned beam antennas are studied by using the IBM 360 digital computer.

This study may be classified in two categories:

(i) Investigation of errors in the solution of the integral equation.

(ii) Computer simulation of the effect of the restricted dynamic range of the measuring system on the accuracy of pattern determination.

The errors in the first category are mainly controlled by the accuracy by which the entries of the integral matrix are evaluated. Also the truncation of the sampling expansion of the unknown pattern contributes to the errors in this category. However, the effect of the truncation error on the integral equation solution is reduced due to the combined filtering action of the phase factor and the synthesized pattern. This is due to the fact that, as the original integration limits are restricted, the contribution of the tails of the truncated composing functions are smaller compared to the case in which the integration range is given by $-\frac{\pi}{2}+\beta_i \leq \psi \leq \frac{\pi}{2}+\beta_i$.

In the evaluation of the entries of the integral matrix, the receiving antenna R is assumed to possess a cosine type aperture amplitude distribution accompanied with a constant phase distribution. Then the pattern of the receiving probe is given by:

$$F^R_{x'}[\sin\theta] = \frac{\cos(kR^R \sin\theta)}{1-\left(\frac{4R^R}{\lambda}\sin\theta\right)^2} \tag{4.20}$$

in which R^R denotes half of maximum linear dimensions of probe R, measured from O' (Fig. 4.1).

The pattern of the synthesized antenna is given by:

$$F^s[\sin\theta] = \frac{\sin\left[kR^s \sin\theta\right]}{\sin\left[\frac{kd}{2}\sin\theta\right]} \tag{4.21}$$

In cases of radiation pattern determination without employing antenna synthesis technique, $F^s[\sin\theta]$ is taken to be equal to unity.

4.3.1. Study of the Accuracy of the Solution of the Integral Equation

The numerical check for the accuracy of the integral equation solution was carried out for various patterns that were assumed to be known.

The numerical investigation was carried out for the following assumed aperture distributions of antenna T,

(i) Uniform aperture distribution with corresponding angular spectrum function,

$$F^T\left[\operatorname{Sin}\psi\right] = \frac{\operatorname{Sin}(kR^T \operatorname{Sin}\psi)}{kR^T \operatorname{Sin}\psi} \tag{4.22}$$

(ii) Cosine aperture distribution with corresponding angular spectrum function

$$F^T\left[\operatorname{Sin}\psi\right] = \frac{\operatorname{Cos}(kR^T \operatorname{Sin}\psi)}{1 - \left(\frac{4R^T}{\lambda} \operatorname{Sin}\psi\right)^2} \tag{4.23}$$

(iii) Cosine squared aperture distribution with corresponding angular spectrum function,

$$F^T\left[\operatorname{Sin}\psi\right] = \frac{\operatorname{Sin}\left[kR^T(\operatorname{Sin}\psi)\right]}{\operatorname{Sin}\psi\left[1-\left(\frac{2R^T}{\lambda} \operatorname{Sin}\psi\right)^2\right]} \tag{4.24}$$

(iv) Cosine aperture distribution with linear phase variation whose corresponding angular spectrum is given by,

$$F^T\left[\operatorname{Sin}\psi\right] = \frac{\operatorname{Cos}\left[kR^T(\operatorname{Sin}\psi - \operatorname{Sin}\theta_{sh})\right]}{1 - \left[\frac{4R^T}{\lambda}(\operatorname{Sin}\psi - \operatorname{Sin}\theta_{sh})\right]^2} \tag{4.25}$$

in which θ_{sh} denotes the angular shift of the pattern due to the effect of the linear phase variation.

The rapidity of variation of the various terms in the integrands of the entries of the integral matrix depends upon the size of the associated parameters R^T, R^s, R^R and ℓ.

The parameter R^T, denoting the maximum linear dimension of the aperture of antenna T, controls the rapidity of variation of the composing functions in the sampling expansion.

The other three parameters R^s, R^R and ℓ determine the behaviour of the functions which exhibit the filtering action. The restricted limits of integration, $\pm\Delta\theta_o$ is determined by the filtering property of these functions. Provided that $\ell \geqslant R^s > R^T$, a good criteria in selecting $\Delta\theta_o$ to maintain stable integral matrix entries, is to choose the first null of the composing function as $\Delta\theta_o$.

If the inequality $R^s > R^T$ holds strongly, the above criteria provides better stability. In the numerical integration procedure, to obatin accurate results, sufficient number of Gaussian abcissa points must be taken depending upon the behaviour of the functions in the integration range. In the investigations in this section, in which the maximum optical size of the measured antenna is taken to be 6λ, a Gaussian quadrature involving 160 abcissa points is utilized.

Table 4.1 gives the mean percentage error in the main-beam and side-lobes for various assumed aperture illuminations as functions of the parameters R^s, ℓ, $\Delta\theta_o$, and (2N+1). In table 4.1, $R^T = 3\lambda$ and the Rayleigh distance for this antenna is 72λ. In all cases the probe is assumed to have a cosine type of aperture distribution given by Eq. 4.20, and its dimension is taken to be

1.5λ). The case of cosine type of assumed aperture distribution is investigated in detail.

The percentage error, ϵ_i is defined as follows,

$$\epsilon_i = 100x \frac{\sum_{n=1}^{N_i} \left| F_A^T(\mathrm{Sin}\psi) - F_c^T(\mathrm{Sin}\psi) \right| / \left| F_A^T(\mathrm{Sin}\psi) \right|}{N} \% \qquad (4.26)$$

where

N_i represents number of samples of percent error in the ith sidelobe (For Table 4.1 N_i=10)

ϵ_i (i = 1, 2, 3) denotes the mean percent error in i^{th} sidelobe

(ϵ_o denotes the mean percent error in the main-beam)

$F_A^T[\mathrm{Sin}\psi]$ is the assumed spectrum of T corresponding to the particular aperture distribution and $F_c^T[\mathrm{Sin}\psi]$ is the spectrum function of T obtained from the integral equation solution.

Near the neighborhood of the nulls of the spectrum functions, as the computer is handling considerably small numbers, the computation error becomes large. Hence, in computing percent errors, the close neighborhoods of such points are not considered.

All the patterns investigated in Table 4.1 are symmetrical around the zero angle. Due to the choice of the measurement angles according to the relation given by Eq. 4.16, the off-diagonal elements of the integral matrix are considerably smaller than the diagonal ones. As it was emphasized before; some off-diagonal elements may then be approximately taken equal to zero to simplify the symmetrical integral matrix. In Table 4.1 the mean error caused by this procedure is compared with the cases in which all elements of the integral matrix are non-zero. This study is given for the cosine type of aperture distribution. N_{nz} denotes the number of non-zero entries which are adjacent to the diagonals.

As observed from the case of cosine type aperture illumination, the mean error increases if all elements of the integral matrix, other than the diagonal terms are taken equal to zero.

On the other hand when the entries of the integral matrix other than two neighboring are equated to zero, error is still not much different than taking all elements as non-zero.

Since the integral matrix is independent of the particular aperture distribution of antenna T, the above argument may be generalized for other types of assumed aperture distributions. Thus, for optically large antennas, the inversion of the integral matrix may be faciliated by taking some of the entries as zero.

Numerical investigations have also shown that by the utilization of more terms in the sampling expansion then the required minimum number, the minima positions of the pattern can be more accurately predicted.

For the cosine aperture distribution Fourier series expansions of $F^T(\sin\psi)$ consisting of 13 and 25 terms are also tried but no convergence was observed.

The results of error study for cosine type assumed aperture distribution with linear phase variation is presented in Table 4.2. In this case, since the pattern is a shifted one, mean errors for sidelobes on both right and left hand sides of the main-beam are given. In Table 4.2 it is assumed that $R^R = 1.5\lambda$ and $R^S = 4.5\lambda$. The parameters are R^T and θ_{sh} which stand for the size of antenna T and the angular shift of the main-beam, respectively. For $R^T = 2.5\lambda$, investigation is made for two different values of ℓ.

As observed from the table, the mean-errors for the positive and negative values of θ_{sh} are nearly identical as expected.

Assumed aperture Distribution of Antenna T	R^s/λ	2N+1	ℓ/λ	$\Delta\theta_o$	N_{nz}	$\epsilon_o\%$	$\epsilon_{-1}\%$	$\epsilon_{-2}\%$	$\epsilon_{-3}\%$
Uniform	10.5	13	6	0.167	all	0.186	0.624	4.713	10.381
Cosine Squared	4.5	13	12	0.167	all	1.387	5.693	10.029	19.341
Cosine	10.5	13	6	0.167	all	0.394	3.705	9.248	17.668
	10.5	13	6	0.167	2	0.466	3.483	9.735	18.078
	10.5	13	6	0.167	0	13.060	20.274	11.548	18.415
	13.5	25	6	0.1	all	0.641	2.613	8.056	15.614
	4.5	13	6	0.167	all	0.434	3.295	11.117	19.684
	4.5	13	6	0.167	2	0.672	4.849	20.180	20.030
	4.5	25	6	0.167	all	0.697	3.762	7.883	15.541
	4.5	13	12	0.15	all	0.455	3.226	7.232	15.725
	4.5	13	40	0.08	all	1.689	3.179	6.617	19.003

Table 4.1 Dependence of the Accuracy of Determined Pattern on Various Parameters

4.3.2. Error Dependence on Dynamic Range of Measuring System

In physical applications of the method for determination of radiation patterns of microwave antennas, the restricted dynamic range of the measuring system is one of the most important factors that determine the accuracy of the results obtained.

It is the purpose of this section to simulate this error on a digital computer.

In the computer simulation, the dynamic range of the near-field response of the synthesized antenna obtained by assuming the presence of a known aperture distribution is restricted by equating the values below a limiting dynamic range to zero. This procedure corresponds to the measurements performed by an experimental set-up having a limited sensitivity.

Table 4.3 gives the dependence of mean percent error in different sidelobes for various values of the parameters DR and $\Delta\theta_o$. (DR represents the dynamic range of the system.) The investigation was made for an assumed cosine distribution with corresponding spectrum function given by Eq. 4.25. Values of the parameters R^T, R^s, R^R, ℓ and (2N+1) are, respectively, equal to 3λ , 4.5λ , 1.5λ , 12λ and 13.

The accuracy by which the unknown angular spectrum function is determined is observed to be strongly depending upon the dynamic range of the measuring system.

4.4. Upper Bound for the Truncation Error in the Sampling Expansion

In the solution of the integral equation for radiation pattern determination, the angular spectrum function $F^T[\sin\psi]$ is approximated by a linear combination of (2N+1) terms of the sampling expansion.

R^T/λ	$\Delta\theta_o$	θ_{sh}	2N+1	ℓ/λ	$\epsilon_{-2}\%$	$\epsilon_{-1}\%$	$\epsilon_o\%$	$\epsilon_1\%$	$\epsilon_2\%$
3	0.167	$-\frac{\pi}{9}$	13	12	29.972	14.816	3.605	2.877	8.483
3	0.167	$+\frac{\pi}{9}$	13	12	8.38	2.863	3.847	15.06	25.41
2.5	0.1	$+\frac{\pi}{9}$	21	12	2.052	0.861	5.767	26.469	128.751
2.5	0.1	$+\frac{\pi}{9}$	21	16	2.022	0.798	5.251	26.561	137.595

$R^R = 1.5\lambda$

$R^S = 4.5\lambda$

Table 4.2 Error Study for Cosine Aperture Distribution with Linear Phase Variation

DR(db)	$\Delta\theta_o$	$\epsilon_o\%$	$\epsilon_{-1}\%$	$\epsilon_{-2}\%$	$\epsilon_{-3}\%$	
20	0.100	15.023	386.938	124.026	84.190	
29	0.100	1.139	13.403	364.959	186.131	
35	0.100	0.650	4.098	20.896	926.811	
41	0.100	0.600	2.755	9.509	29.798	$R^T = 3\lambda$
50	0.100	0.572	3.021	7.295	17.814	$R^S = 4.5\lambda$
20	0.167	6.077	54.765	79.552	121.103	$R^R = 1.5\lambda$
29	0.167	1.331	16.131	79.804	221.033	$\ell = 12\lambda$
35	0.167	0.458	4.898	21.901	249.211	2N+1 = 13
41	0.167	0.451	3.074	9.376	28.682	
50	0.167	0.412	3.043	7.501	17.396	

Table 4.3 Dependence of Error on Dynamic Range

The number of terms to be used in the expansion depends upon the rate of change of the function $F^T[\mathrm{Sin}\psi]$. Higher this rate of change, more is the required number of terms to achieve a desired accuracy. On the other hand, the maximum rate of variation depends upon the maximum optical size of the radiating aperture. Therefore, the error introduced due to the truncation of the series is proportional to the maximum optical size of the aperture.

With $s_2 = \mathrm{Sin}\psi$, the upper bound for the mean-square error, $|e_N(s)|^2$, in the truncated sampling expansion of the angular spectrum function of antenna T is given by; (See p.183-184 [PAP])

$$|e_N(s_2)|^2 \leqslant \frac{WkR^T}{\pi} \sum_{|n|>N} \frac{\left\{\mathrm{Sin}\left[kR^T(s_2-nP)\right]\right\}^2}{\left\{kR^T(s_2-nP)\right\}^2} \qquad (4.27)$$

where W is the energy of the function $F^T[\mathrm{Sin}\psi]$ and is given by;

$$W = \int_{-\infty}^{\infty} |F^T(s_2)|^2 \, ds_2 = \frac{1}{2\pi} \int_{-kR^T}^{kR^T} |E_x(y)|^2 d(ky) \qquad (4.28)$$

The function $E_x(y)$ corresponds to the aperture electric field distribution of antenna T which is equal to the inverse Fourier transform of the angular spectrum function.

Hence, when $F^T(s_2)$ is approximated by (2N+1) terms of the sampling expansion, the mean-square error for any s_2 is bounded by the expression given in Eq. 4.27. As it can be observed from Eq. 4.27, for optically large antennas, the mean-square truncation error depends on the number of terms utilized and on the maximum linear dimensions of the antenna.

V. EXPERIMENTAL INVESTIGATIONS

In this chapter a detailed experimental investigation for the determination of radiation-patterns of fanned-beam antennas is presented. Both the transmitting antenna whose pattern is to be determined and the measuring probe are chosen to be H-plane sectoral horn antennas which possess narrow beams in the H-plane and relatively much wider beams in the E-plane. Deliberately blocking the aperture of the measured antenna by means of inserting a metal piece into its aperture, a wide variety of fanned-beam patterns is generated from a single horn. Thus, it is possible to experimentally verify the theory developed in the preceeding chapters of this thesis for various types of radiation-patterns.

In the solution of the integral equation, for radiation-pattern determination, the receiving probe is assumed to possess a cosine aperture electric field distribution.

The dynamic range of the near-field measuring system is about 25 db. But, as it was studied in Section 4.3 associated with the numerical investigations, the restricted dynamic range presents a big problem in the prediction of the low-level side-lobes. Thus, aperture blocking, besides providing a large variety of radiation-patterns, also serves to increase the side-lobe levels to overcome the restricted dynamic range handicap in the experimental verification of the theory. However, it should be noted that radiation patterns having dominant sidelobes generally is not desired. However, here such patterns are purposefully utilized to overcome the dynamic range problem.

5.1. Description of the Measurement Set-Up's

The circuit diagram of near-field measurement set-up utilized in the laboratory is given in Fig. 5.1.

A varian X-13 Klystron is used as the X-band source. A reference signal is taken from the source using a 20 db cross coupler. A calibrated attenuator and a calibrated phase shifter is inserted in the path of the reference signal. This signal is mixed with the received signal in a T-section and then the mixed signal is detected. The isolators at both ends of the T-section serve the purpose of preventing the penetration of the signal received by the probe into the reference arm and vice versa. The output is observed on the meter of the VSWR-amplifier.

The relative amplitude and phase of the received signal is measured by adjusting the calibrated attenuator and the phase shifter to obtain a minimum. The relative amplitude and phase are directly read from the dial of the attenuator and the phase shifter.

The signal measured for the positions of antennas T and R in which their aperture unit normal vectors are colinear corresponds to the reference value of received signal. All other measured signals are defined w.r.t this reference signal. The coarse variable attenuator in the reference arm serves the purpose of adjusting the amplitude of the reference received signal to a desired level.

Initially, at the reference position both antennas are tuned to obtain maximum received signal, i.e., minimum VSWR.

Antenna T is rotated about its aperture center. To avoid phase errors due to cable bending, a coaxial rotary-joint is employed in the feed-system of T. The angular position of T is observed from a scale which is mounted on the rotating part of the antenna rotator.

To enable antenna synthesis, the receiving probe is mounted on the vertical supporting bar of a carriage which slides over two parallel circular bars. Also, a mechanism for holding microwave absorbing plates is provided on the vertical supporting bar. Thus, by covering the supporting structure and the tuning components of the probe, except its aperture, by absorbing material, the multiple reflections between the transmitting and receiving structures are minimized. The study of the axial field of antenna T shows that the interaction between the transmitting and receiving antennas is negligible in the Fresnel region of antenna T. The carriage can provide the probe R, about 80 cm of linear movement.

The modulating 1 KHz square wave signal can cause the klystron to give output at two different frequencies. This undesired effect is checked for by observing part of the detected klystron output on the screen of an oscilloscope. For this purpose a 20 db directional coupler is inserted in the main signal path of antenna T. Then the source is tuned so that only a single frequency output exits.

In performing the near-field measurements, environmental objects that may give rise to reflections are covered with microwave absorbing plates. In the 25 db dynamic range, the phase measurement error is within $\pm$ 5 degrees, and the amplitude measurement error within $\pm$ 0.5 db.

In making far-field radiation-pattern measurements a conventional circuit shown in Fig. 5.2 is utilized. In each reading, corresponding to a different angular position of antenna T, the calibrated attenuator is adjusted to yield a specific fixed output on the VSWR indicator. Then the relative levels of the power pattern are directly read from the scale of the calibrated attenuator. Again microwave absorbing plates are placed at critical positions to avoid reflections.

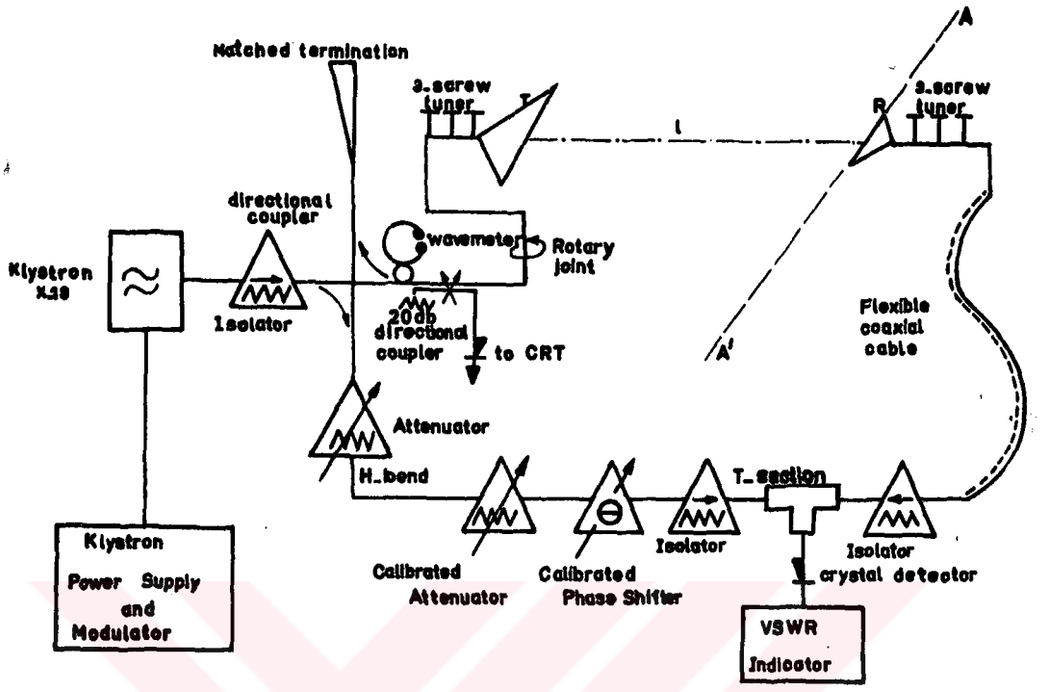

Fig. 5.1 Set-Up for Near-Field Measurements

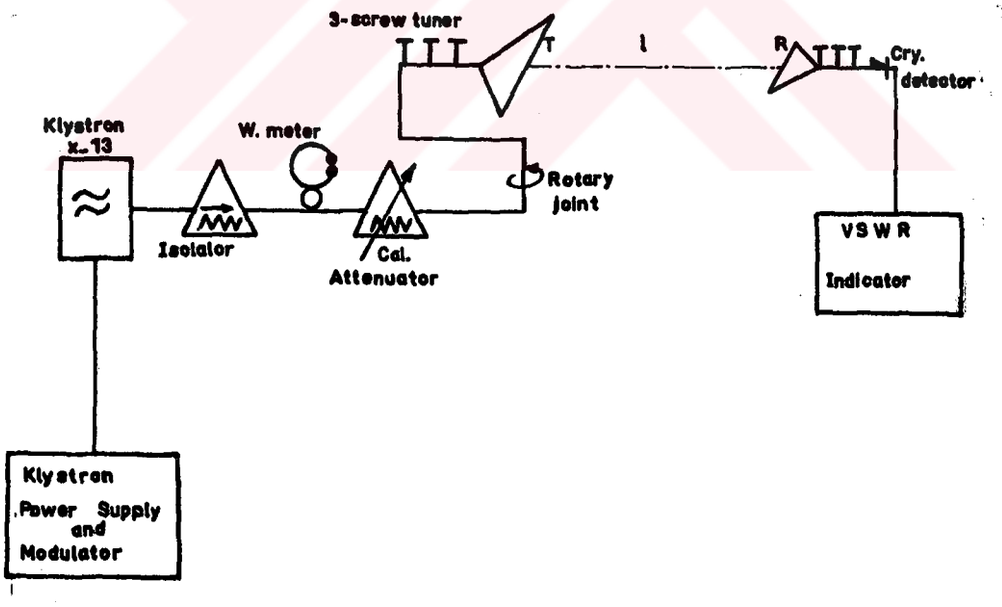

Fig. 5.2 Set-Up for Far-Field Measurements

The seperation between the measured and measuring antennas are usually taken to be considerably larger than the Rayleigh distance for antenna T.

5.2. Determination of H-Plane Radiation-Patterns of Fanned-Beam Antennas

In this section the determination of radiation-patterns of H-plane sectoral horn antennas having fanned-beams are considered. The theory presented in Chapter IV is utilized to determine the H-plane patterns. The horns used in the experiments are built such that the dimension in the H-plane is considerably greater than the E-plane dimension which is equal to the smaller size of the waveguide, WG16. Certain part of the horn apertures are blocked by metal pieces to produce different radiation-patterns.

In order to show the reproducible property of the results, the same far-field pattern is predicted from different near-field measurements performed at distinct distances.

To show the validity of the statement, that, "the integral matrix evaluated for an antenna of specific optical-size can be used for antennas of smaller optical sizes as well", the integral matrix evaluated for the 18 cm horn was used to predict the far-field pattern of the 12 cm horn also.

Patterns predicted with an without employing antenna synthesis are plotted on the same graph to demonstrate the importance of antenna synthesis. (Fig. 5.6)

Plots of the same predicted pattern obtained using different number of terms, NN, [NN=2N+1] in the sampling expansion of the unknown are given. (Figs. 5.3, 5.4, 5.5, 5.6, 5.7, 5.8)

The necessity of integral equation solution is demonstrated by plotting the direct response of the synthesized antenna on the same graph showing the directly measured far-field pattern and the one obtained from integral equation solution. (Figs. 5.6 and 5.8)

Different size measuring probes are utilized to predict the same pattern in order to show that in the theory developed, the directivity of the probe is taken into account.

Direct far-field measurements are performed using two different probes to indicate that the probe directivity, in far-field pattern measurements, can give rise to errors specially in the sidelobe regions [BR 2].

5.2.1. Determination of the Radiation-Pattern of 18 cm H-Plane Sectoral Horn with Central Aperture Blocking

The far-field radiation pattern of a 18 cm (y-dimension) H-plane Sectoral Horn (HPSH) antenna whose aperture was blocked by a 6.5 cm metallic ribbon was predicted from near-field measurements performed at a distance, ℓ = 47.6 cm. The klystron was tuned to a frequency f = 9.948 GHz. The half size, R^R, of the receiver HPSH probe was 4.5 cm. Plots of predicted far-field radiation patterns obtained using both NN = 13 and NN = 25 terms in the sampling expansion are given in Fig.5.3. For comparison, plot of the H-plane far-field pattern directly measured at the far-field of the antenna is plotted in the same figure. The direct measured far-field pattern by no means completely represents the true radiation pattern at infinity, since the pattern measured at a finite distance depends upon the size of measuring probe [BR 2], and some undesired reflections

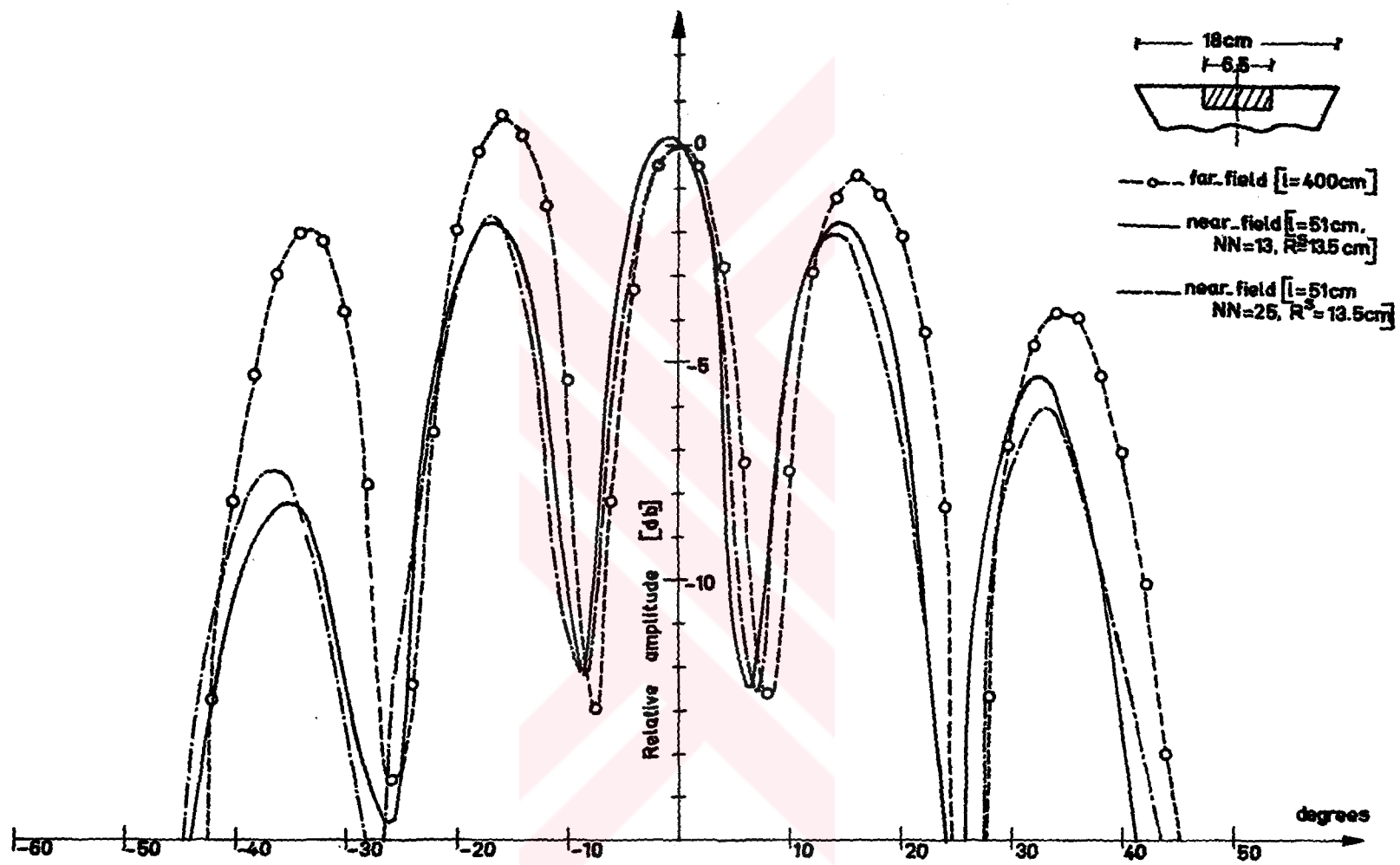

Fig. 5.3 Patterns of 18cm H P S H antenna with central aperture blocking

from environmental objects can still exist in spite of the microwave absorbing plates placed at some critical points. However, still a good basis for checking the predicted patterns is provided by means of this comparison.

From Fig. 5.3 it can be observed that the patterns calculated using 13 and 25 terms are not much different which agrees with the discussion given in the numerical investigations. (table 4.1).

The agreement between the directly-measured and predicted far-field patterns is better in the main beam and in the first sidelobes, but not so better in the second sidelobes. The positions of the minima and maxima of the pattern are observed to be more accurately determined in the case where 25 terms in the sampling expansions are used.

5.2.2. Determination of the Radiation-Pattern of 18 cm H-Plane Sectoral Horn with Off-Central Aperture Blocking

Far-field pattern of the 18 cm HPSH whose aperture was blocked by a metal piece of 6.5 cm long replaced in an off-center position was determined from near-field measurements performed at a distance, ℓ, of 47.6 cm. The source was tuned to a frequency of f = 9.7GHz. The main beam of the antenna appears slightly shifted to the right; i.e., to positive angles.

Predicted patterns obtained by employing 13 and 25 terms in the sampling expansion are plotted in Fig. 5.4. For comparison the direct measured far-field pattern is also plotted on the same graph. A very good agreement between the direct-measured and predicted patterns is obtained for angles in the range of $\pm 30^{\circ}$. For larger angles, the pattern obtained using 25 terms follows the direct-measured far-field pattern very closely.

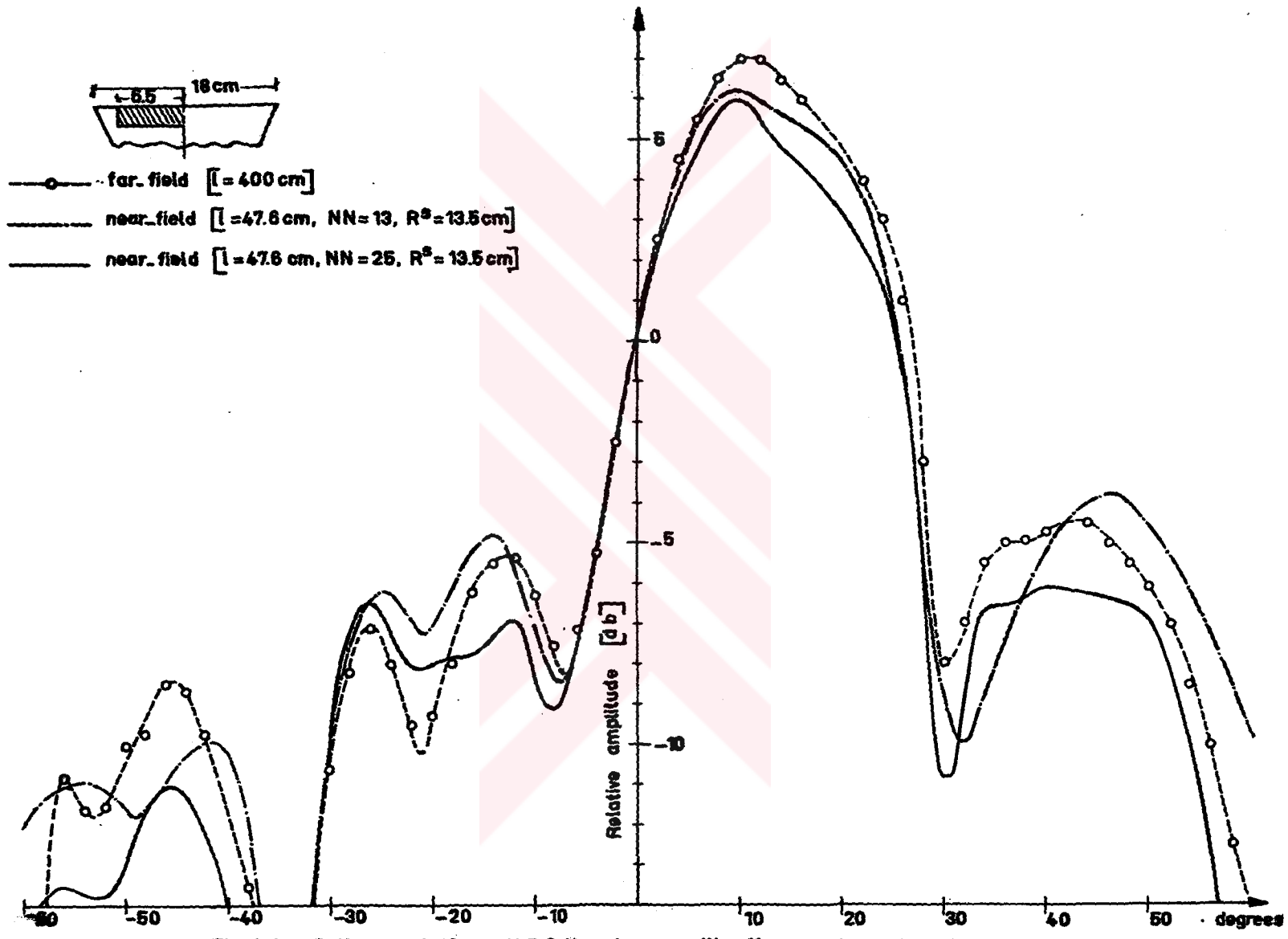

Fig. 5.4 Patterns of 18 cm H P S H antenna with off_central aperture blocking

Tolarances in near-field amplitude and phase measurements and reflections from environmental objects are some of the factors which are responsible for the discrepancies between the predicted and direct measured patterns. Some other causes of the disagreement may be due to the inconsistency of the far-field pattern obtained from measurements utilizing different size probes and due to inaccuracies in integral equation solution for radiation pattern determination.

In performing both the far-field and the near-field measurements an HPSH receiving probe of R^R = 4.5 cm was utilized.

5.2.3. Determination of the Radiation-Pattern of 12 cm H-Plane Sectoral Horn with Central Aperture Blocking

Predicted far-field radiation patterns of a 12 cm centrally blocked 12 cm HPSH antenna obtained from near-field measurements, performed at distances ℓ = 59.8 cm and ℓ = 47.6 cm, are plotted in Fig. 5.5.

A R^R = 4.5 cm HPSH probe was utilized and the half-size of the aperture of the synthesized antenna was R^S = 13.5 cm. The klystron was tuned to a frequency of 9.867 GHz.

The predicted patterns were obtained by assuming that the optical size of antenna T was 6λ . Thus the integral matrices computed in the determination of far-field patterns in Figs. 5.3, 5.4 and 5.5 from measurements at ℓ = 47.6 cm, are identical. This illustrates the fact that the integral matrix computed for an antenna of certain optical size may be used in the estimation of far-field patterns of smaller optical size antennas as well.

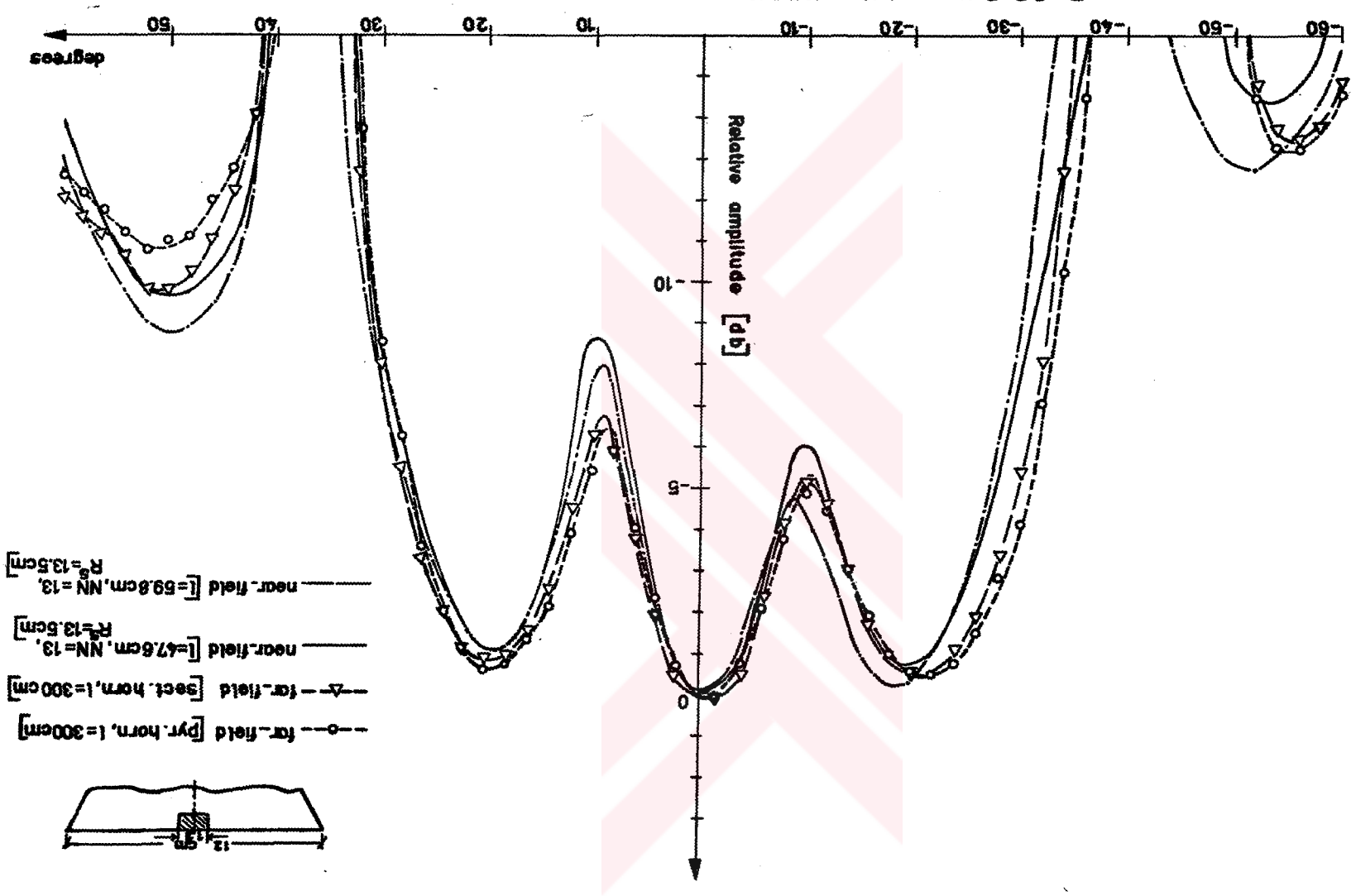

Fig. 5.5 Patterns of 12cm HPSH antenna with central aperture blocking

Direct far-field measurements were performed at the same distance using both the 9 cm HPSH probe and also the 7.5 cm x 7.5 cm Sanders pyramidal horn. A good agreement between the two direct measured patterns is obtained for small angles. The agreement for the larger angles is smaller being in agreement with Brown's work [BR 2] . The disagreement between the predicted and direct measured patterns is not much larger than the disagreement between the two distinct direct measured curves. But of course, additional errors may be introduced into the predicted patterns due to various factors mentioned in the preceeding sections.

In Fig. 5.6, the far-field patterns predicted without employing antenna synthesis are plotted. In obtaining these patterns the same integration limits in the case with the antenna synthesis were utilized. The predicted pattern obtained using 25 terms in the sampling expansion exhibits much better agreement than the one obtained using 13 terms. As pointed out in the earlier chapters, to obtain the same degree of accuracy; the integration limits for the integrals constituting the entries of the integral matrix should be taken much larger. This, of course, implies more computational work.

The far-field pattern was also predicted from near-field measurements performed employing a large (R^R = 9 cm) HPSH probe. The half size of the aperture of the synthesized antenna is therefore 27 cm. In this case, as the pattern of the synthesized antenna has a narrower beam than pattern synthesized using a R^R=4.5 cm receiving horn, the integration limits could be further reduced. But in that measuring range (ℓ = 47.6 cm) since the measuring probe was too large (even larger than the measured antenna), the interaction between the measured and measuring antennas was large. Thus the disagreement between the predicted and direct measured patterns,

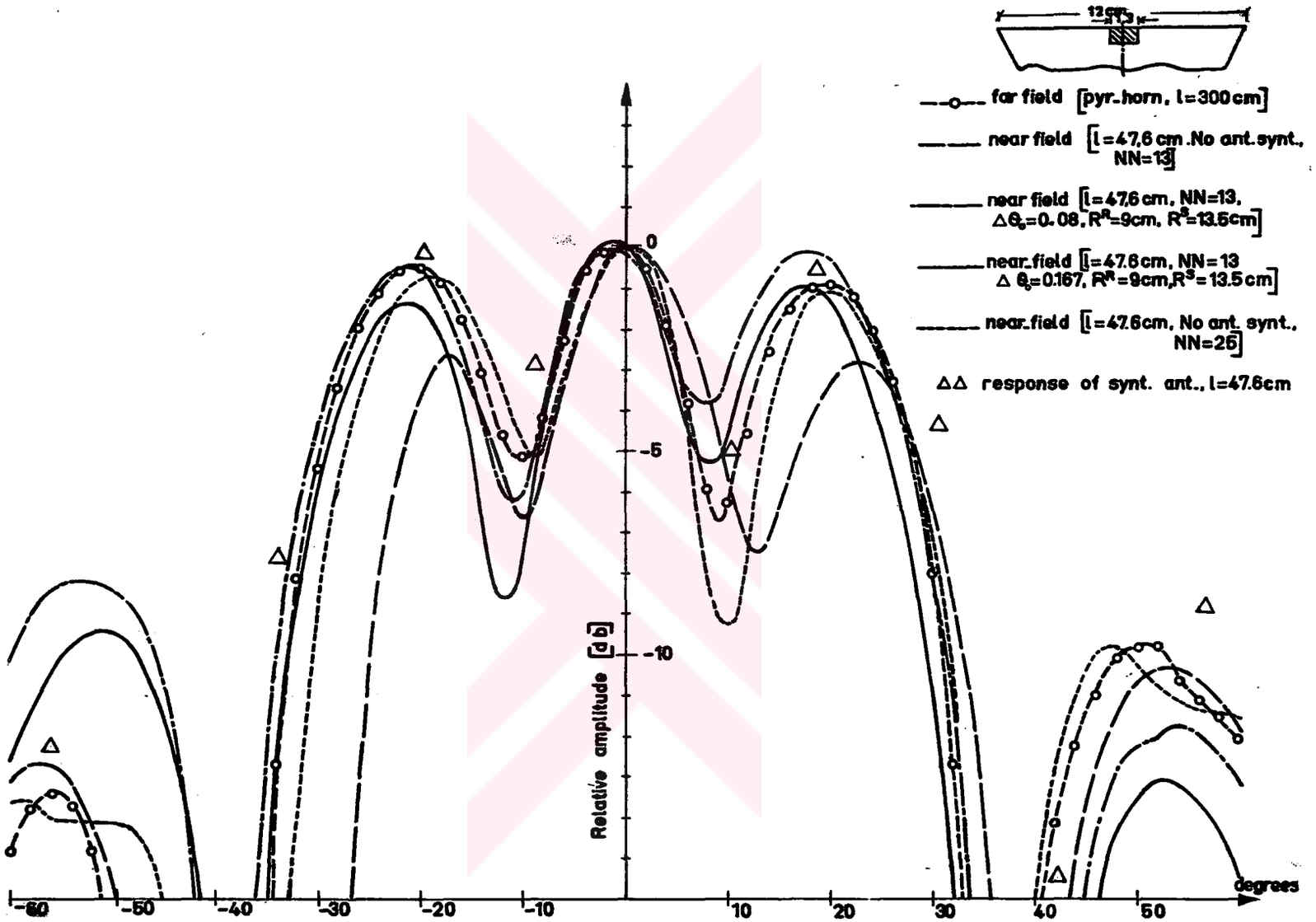

Fig.5.6 Patterns of 12 cm H P S H antenna with central aperture blocking.

specially in the sidelobe regions, is large. Therefore, in order to minimize the interaction and at the same time to reduce the computational work, it is more advantageous to use a small measuring probe and synthesize a large antenna. But if the seperation, d, between the probe positions on contour AA' in Fig. 4.1 is too large, then the synthesized pattern will contain more than one main-beam. Then in the evaluation of the entries in the integral matrix, the integration need be considered over more than one integration range.

The near-field response of the R^S = 27 cm synthesized antenna is also plotted in Fig. 5.6. The optical size of synthesized antenna is 4.5 times larger than the optical size of the measured antenna T. According to Martsafey [MAR], this direct response will yield the far-field pattern. But it is obvious that the pattern obtained through integral equation solution is much more accurate and moreover a continuous pattern is predicted from 13 discrete values of the near-field response of the synthesized antenna.

5.2.4. Determination of the Radiation-Pattern of 18 cm H-Plane Sectoral Horn with Off-Central Aperture Blocking

Far-field pattern of 18 cm HPSH antenna whose aperture was blocked by a 6.5 cm metal piece located off-center as shown in Fig. 5.7, was predicted using the near-field data obtained at distances ℓ = 47.6 cm and ℓ = 55.2 cm. The source was tuned to a frequency of f = 9.87 GHz. In Fig. 5.7 the predicted patterns obtained using 13 termsin the sampling expansion of F_x^T [Sinψ] and the directly measured far-field pattern are plotted. In measuring the far-field pattern directly, the same probe of R^R = 4.5 cm HPSH used in the near-field measurements was utilized.

In an other measurement for small angles a good agreement between the direct-measured and predicted patterns is obtained. Agreement is less for large angles. For the majority of angles utilized the two predicted patterns obtained from near-field measurements at different distances agree quite well. This conclusion indicates that the pattern obtained through integral equation solution is independent of the measurement distance. But naturally the distance ℓ, as pointed out in Chapter III, need be greater than some minimum value which is the Rayleigh distance for the E-plane aperture dimension. The satisfactory agreement obtained between the predicted curves is also an indication of the fact that the measurements in the available dynamic range are accurate.

The predicted patterns obtained using 25 terms in the sampling expansion of the unknown are plotted in Fig. 5.8. Direct far-field measurements at the same distance were performed using two different receiving probes; the 9 cm HPSH and the Sanders pyramidal horn. These patterns are also plotted in Fig. 5.8.

The half-size of the H-plane dimension of the aperture of the synthesized antenna was R^s = 13.5 cm; i.e., 1.5 times larger than the optical size of the aperture of antenna T. Direct near-field responses of the synthesized antenna obtained both at ℓ = 47.6 cm and ℓ = 55.2 cm are plotted in Fig. 5.8. These plots give some idea about the general nature of the far-field pattern but obviously are too approximate. Hence the size of the synthesized antenna is not large enough to yield a good representation of the desired patterns. The importance of the integral equation solution becomes very clear here. Feeding the near-field response of synthesized antenna to the computer for integral equation solution, the continuous predicted patterns in Fig. 5.7 and Fig. 5.8 are obtained which represent the far-field radiation pattern quite accurately.

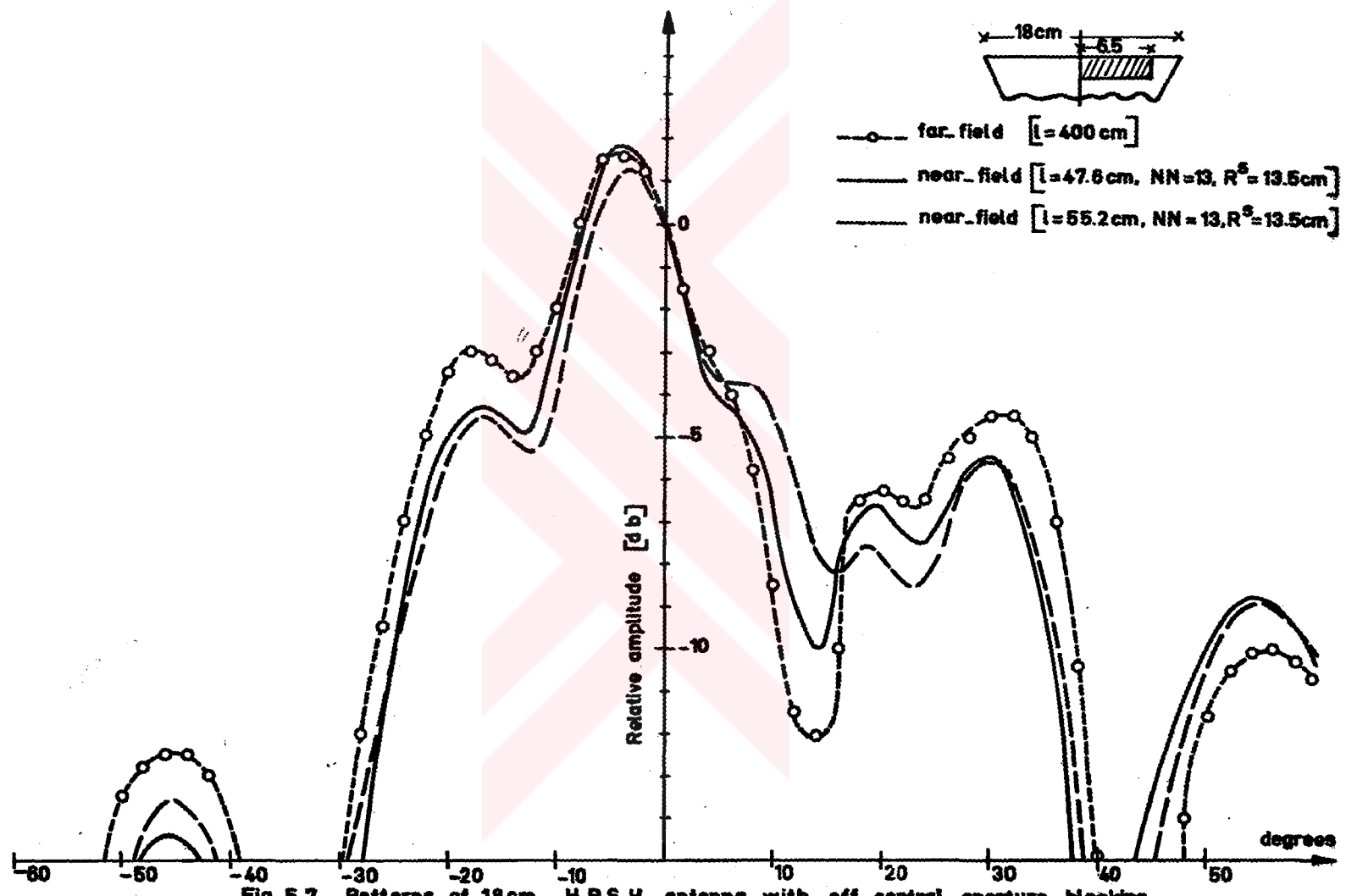

Fig. 5.7 Patterns of 18cm H P S H antenna with off_central aperture blocking

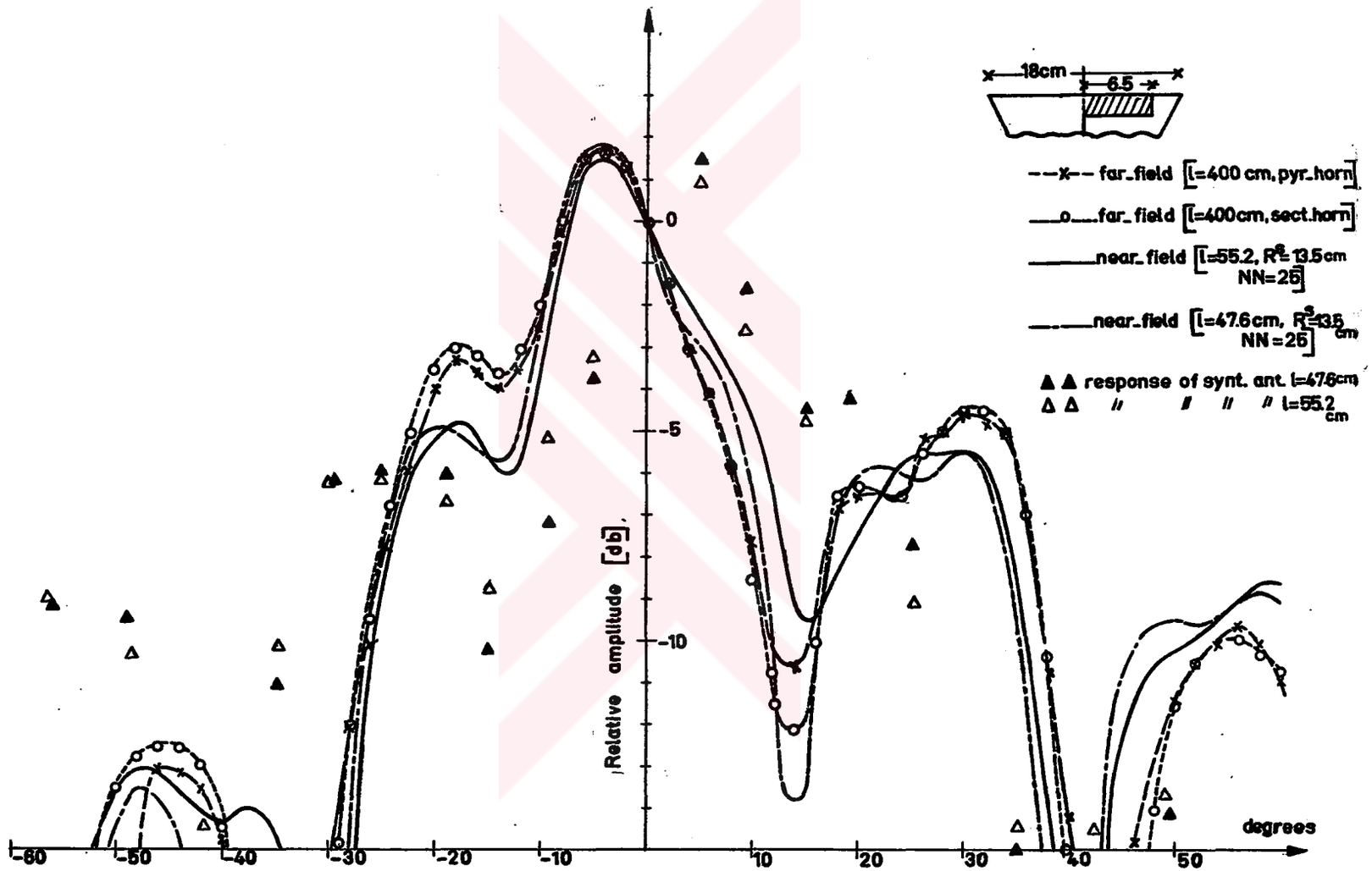

Fig. 5.8 Patterns of 18 cms. H PS H antenna with off_central aperture blocking

5.3. About Errors in the Predicted Patterns

One of the most important sources of error in obtaining radiation patterns from near-field measurements is the limited dynamic range. Evidently in order to overcome that problem, powerful sources and sensitive microwave receivers with high signal to noise ratios must be utilized. The same discussion also applies for the direct far-field measurements.

Undesired reflections from the environmental objects are also serious sources of error. To a certain extent such reflections may be prevented by the utilization of microwave absorbing material.

Utilization of a oversize receiving probe can give rise to errors; as such a probe may be distorting the field seriously. This effect can be clearly seen in Fig. 5.6 from the curve giving the predicted pattern obtained using a R^R = 9 cm HPSH probe.

The mechanical system associated with the near-field measuring set-up must be as accurate as possible since the near-field measurements are performed at pre-fixed angular positions of antenna T. If the mechanical aligning is inaccurate, the mathematical formulation and the experimental model will not be consistent and this will give rise to severe errors in the predicted patterns. For example, if in the antenna synthesis procedure, the receiving probe does not move on a contour which is parallel to the aperture of antenna for the position $\beta_i = 0$, but, makes a small angle with the true contour AA' in Fig. 4.1, then effectively the measurements would have been performed at angles different than the pre-fixed ones. But still the computer evaluates the integral matrix as if the measurements were made at the pre-fixed β_i's. This, of course causes errors in the predicted patterns. On the other hand inaccurate angular positioning of antenna T and incorrect angle measuring dials also give rise to serious errors.

A study of the errors mentioned above was made by allowing the β_i's in the integral matrix to be different then the pre-fixed angles according to a sinusoidal law. That is to say, the error in β_i's was assumed to vary sinusoidally being zero at 0° and maximum at $\pm 90^\circ$. The maximum error present in the pre-fixed β_i's was assumed to be $\pm 2^\circ$. The results indicate clearly that errors of the order of ± 1 db in sidelobe regions can be obtained due to these inaccurate geometrical alignments.

In near-field measurements to prevent the phase errors due to the cable bendings, the rotary-junctions can be utilized. With the present near-field measuring set-up the coaxial cable at the receiving end was kept long in order to minimize the cable bending.

In direct far-field pattern measurements, as it was pointed out several times, the patterns obtained by using different size receiving probes can be different. Also the reflections from the environmental objects causes errors. In practice, the measurement distance is usually kept sufficiently large and a probe with moderate directivity characteristics is used to overcome the problem of undesired reflections from the environment.

VI. CONCLUSIONS

A general transmission formula, which gives the phase and amplitude of the received signal at a reference cross-section in the waveguide of the receiving probe, when illuminated by a transmitting antenna, is derived. The formula is general with regard to the type of aperture electric field polarizations of the two antennas, and their positioning w.r.t each other.

Making use of this general transmission equation, a simple and rigorous method for correcting the errors in Fourier transform method of far-field radiation pattern prediction [RAM] is proposed. It is shown that, if the directive property of the measuring probe is overlooked, then the predicted pattern may contain considerably large errors. (Specially in the sidelobe regions if the probe possesses a pattern having its principal maximum at zero degrees.)

The general transmission formula is also used to show that the response of a plane array can be synthesized from measurements performed over a plane surface. Antenna synthesis technique, as it reduces the necessary computational work and improves the accuracy of the predicted pattern, is proven to be of great importance.

The use of sampling theorem enables the unknown spectrum function to be represented by a minimum number of terms with quite good accuracy. The minimum number of terms that must be used in the expansion is determined by the largest optical size of the aperture of the measured antenna.

Numerical investigations show that the accuracy of the integral equation solution, attained even by employing a minimum sampling rate expansion is satisfactory. Making the measurements at some pre-selected angles, some off-diagonal entries of the integral matrix become negligible. Hence, as shown in Table 4.1 these entries can be taken as zero without much affecting the accuracy of the predicted patterns. Further, investigation can be carried out on this point as the prediction of far-field patterns of very large optical size antennas will require the evaluation and inversion of very large matrices.

H-plane radiation patterns of various HPSH-antennas are predicted using the theory developed in this thesis. Very satisfactory agreement between the predicted and direct-measured far-field patterns is obtained.

The method is observed to be sensitive to geometrical alignment. Small errors (such as $\pm 2^{o}$) in angular positionings can give rise to considerably large errors in the predicted pattern of the order of $\pm$ 1 db.

The integral matrix computed for an antenna of specific optical-size can be used to predict the far-field patterns of smaller optical-size antennas as well. Therefore, some standard "inverse integral matrices" can be prepared for the prediction of radiation patterns of antennas which range between specific optical-sizes. The entries of such integral matrices will be determined by the maximum optical size of measured antenna, angular spectrum function of receiving probe, pattern of synthesized antenna and seperation between the measured and synthesized antennas. Then the multiplication of the "measurement matrix" with the "inverse integral matrix" will be what it is needed to determine the unknown sampling expansion coefficients which in turn will yield the unknown angular spectrum function.

One obvious advantage of obtaining far-field patterns from near-field measurements is that at near distances to the antenna, as the field strength is high, measurements will be easy to perform. However, if one gets too close to the antenna, interaction becomes a problem. Therefore, a topic of further study can be an attempt to account for the interaction problem. For the moment this seems to be a very complicated boundary value problem to solve. Usually every precaution is taken to prevent this undesired phenomenea.

The proposed theory is also applicable without synthesizing an antenna; but as emphasized quite often in this thesis, the computational work in evaluating the integral matrix will be more.

Another subject of further investigation can be the effect of synthesizing arrays with different patterns; especially ones having very low sidelobes. In other words, if, in the measurement, specific attenuations and phase shifts are given to the signal received by the probe, at its different locations on the measurement plane, then the synthesized pattern may be caused to have low sidelobes. Then the action of restricting the original integration range will be more valid and hance the integral equation solution more accurate.

It was observed in Section 3.3 that the pattern of the synthesized antenna, in the limiting case of infinite size aperture, behaves as a delta function. This fact suggests that, with some degree of approximation, radiation patterns of optically-large antennas may be determined from near-field amplitude measurements only. This however requires further investigations.

APPENDIX I: DERIVATION OF THE EXPRESSION FOR THE GENERAL ELECTROMAGNETIC FIELD IN TERMS OF ANGULAR SPECTRUMS

For the radiating antenna T, shown in Fig. 2.1 the three components of the E-field are given by Eqs. 2.3, 2.4 and 2.5. The angular spectrum functions F_x and F_y are obtained from Eqs. 2.1 and 2.2 respectively. Then F_z, in the source free region $z > 0$, can be obtained from the divergence condition $\bar{\nabla}.\bar{E} = 0$. Thus;

$$\bar{\nabla}.\bar{E} = \int_{-\infty}^{\infty}\int_{-\infty}^{\infty}\left[F_x \frac{\partial}{\partial x}(e^{-j\bar{k}.\bar{r}}) + F_y \frac{\partial}{\partial y}(e^{-j\bar{k}.\bar{r}}) + F_z \frac{\partial}{\partial z}(e^{-j\bar{k}.\bar{r}})\right] ds_1 ds_2 = 0 \qquad (A.1.1)$$

Since $\exp\left[-j\bar{k}.\bar{r}\right] = \exp\left[-jk(s_1x+s_2y+cz)\right]$, Eq. A.1.1 reduces to

$$\bar{\nabla}.\bar{E} = -jk\int_{-\infty}^{\infty}\int_{-\infty}^{\infty}\left[F_x s_1+F_y s_2+F_z c\right] e^{-j\bar{k}.\bar{r}}\, ds_1 ds_2 = 0 \qquad (A.1.2)$$

This equation is satisfied if one takes

$$F_z(s_1,s_2) = -\frac{1}{c}\left[s_1F_x(s_1,s_2)+s_2F_y(s_1,s_2)\right] \qquad (A.1.3)$$

which is the required expression for the angular spectrum function F_z. Hence the expression for the $\bar{E}$-field is;

$$\bar{E}(x,y,z) = \int_{-\infty}^{\infty}\int_{-\infty}^{\infty}\left[cF_x\bar{e}_x+cF_y\bar{e}_y-(s_1F_x+s_2F_y)\bar{e}_z\right] e^{-j\bar{k}.\bar{r}}\, \frac{ds_1 ds_2}{c} \qquad (A.1.4)$$

Similarly the expression for the $\bar{H}$-field follows from the curl expression: $\bar{\nabla}x\bar{E} = -jw\mu\bar{H}$, or

$$H_x = -\frac{1}{jw\mu}\left(\frac{\partial E_z}{\partial y} - \frac{\partial E_y}{\partial z}\right) \qquad (A.1.5)$$

$$H_y = \frac{1}{jw\mu}\left(\frac{\partial E_z}{\partial x} - \frac{\partial E_x}{\partial z}\right) \qquad (A.1.6)$$

$$H_z = -\frac{1}{jw\mu}\left(\frac{\partial E_y}{\partial x} - \frac{\partial E_x}{\partial y}\right) \qquad (A.1.7)$$

Then utilizing Eq. A.1.4 in Eqs. A.1.5, A.1.6 and A.1.7 we obtain,

$$\bar{H}(x,y,z) = Y_o \int_{-\infty}^{\infty}\int_{-\infty}^{\infty}\Big\{\left[-s_1 s_2 F_x - (s_2^2+c^2)F_y\right]\bar{e}_x + \left[(s_1^2+c^2)F_x + s_1 s_2 F_y\right]\bar{e}_y$$

$$+ \left[-cs_2 F_x + cs_1 F_y\right]\bar{e}_z\Big\}\, e^{-j\bar{k}.\bar{r}}\,\frac{ds_1 ds_2}{c} \qquad (A.1.8)$$

where Y_o denotes the characteristic admittance of free space.

APPENDIX II: EVALUATION OF THE ASYMPTOTIC FAR-FIELD FORM OF Eq. 2.17 BY THE METHOD OF STATIONARY PHASE

Using the expressions of x'; y'; z' in terms of polar coordinates $(r', \theta_o', \varphi_o')$; Eq. 2.17 can be written as

$$\bar{E}(\bar{r}') = \int_{-\infty}^{\infty}\int_{-\infty}^{\infty}\left[F^R_{x'}\bar{e}_{x'} + F^R_{y'}\bar{e}_{y'} - \frac{1}{c'}\left(s_1' F^R_{x'} + s_2' F^R_{y'}\right)\right] e^{-jkr'\left[s_1'\ell_o + s_2' m_o + c' n_o\right]} ds_1' ds_2' \qquad (A.2.1)$$

where $\ell_o = \sin\theta_o' \cos\varphi_o'$, $m_o = \sin\theta_o' \sin\varphi_o'$, $n_o = \sqrt{1-\ell_o^2-m_o^2} = \cos\theta_o'$

and $c' = \sqrt{1-s_1'^2 - s_2'^2}$.

Assuming that the condition $kr' \gg 1$ is fullfilled, an integral, I, can be represented by the first term of the stationary phase method of integration [PAP] , as shown below;

$$I = \int_{-\infty}^{\infty}\int_{-\infty}^{\infty} g(s_1', s_2') e^{-jkr'\mu(s_1', s_2')} ds_1' ds_2' \approx \frac{-2\pi\sigma\, e^{j\frac{\pi}{2}}}{\sqrt{|\alpha\beta - \gamma^2|}} \frac{e^{-jkr'\mu(s_{1o}', s_{2o}')}}{kr'} \qquad (A.2.2)$$

where (s_{1o}', s_{2o}') are called the critical points of the first kind obtained from;

$$\frac{\partial\mu}{\partial s_1'} = \frac{\partial\mu}{\partial s_2'} = 0 \qquad (A.2.3)$$

and

$$\alpha = \left.\frac{\partial^2 \mu}{\partial s_1'^2}\right|_{s_{1o}', s_{2o}'}, \quad \beta = \left.\frac{\partial^2 \mu}{\partial s_2'^2}\right|_{s_{1o}', s_{2o}'}, \quad \gamma = \left.\frac{\partial^2 \mu}{\partial s_1' \partial s_2'}\right|_{s_{1o}', s_{2o}'} \tag{A.2.4}$$

also

$$\sigma = \begin{cases} +1 & \text{if} \quad \alpha\beta > \gamma^2 \quad \text{for} \quad \alpha > 0 \\ -1 & \text{if} \quad \alpha\beta > \gamma^2 \quad \text{for} \quad \alpha < 0 \\ -j & \text{if} \quad \alpha\beta < \gamma^2 \end{cases} \tag{A.2.5}$$

Since in Eq. A.2.1,

$$\mu(s_1', s_2') = s_1' \ell_o + s_2' m_o + \sqrt{1 - s_1'^2 - s_2'^2}\; n_o \tag{A.2.6}$$

from Eq. A.2.3 one obtains

$$\begin{aligned} s_{1o}' &= \ell_o \\ s_{2o}' &= m_o \\ c_o' &= n_o \end{aligned} \tag{A.2.7}$$

and from the set of equations in Eq. A.2.4,

$$\alpha = -\left(1 + \frac{\ell_o^2}{n_o^2}\right), \qquad \beta = -\left(1 + \frac{m_o^2}{n_o^2}\right), \quad \gamma = -\frac{m_o \ell_o}{n_o^2} \tag{A.2.8}$$

Furthermore Eq. A.2.5 yields $\sigma = -1$.

Therefore using Eqs. 2.18, A.2.1, A.2.2, A.2.6, A.2.7, A.2.8 and with $\ell_o \rightarrow s_1'$, $m_o \rightarrow s_2'$, $n_o \rightarrow c'$, one obtains

$$\bar{E}_R(\bar{r}')\Big|_{\text{far field}} = 2\pi c' \, e^{j\frac{\pi}{2}} \frac{e^{-jkr'}}{kr'} \Big\{ F_{x'}^R \, \bar{e}_{x'} + F_{y'}^R \, \bar{e}_{y'} - \frac{1}{c'}\left[s_1' F_{x'}^R + s_2' F_{y'}^R\right] \bar{e}_{z'} \Big\} \tag{A.2.9}$$

APPENDIX III: SAMPLING EXPANSIONS FOR $F_x^T(s_1,s_2)$ AND $F_y^T(s_1,s_2)$

Let the aperture of antenna T in Fig. 3.2 be denoted by A_T. A_T is contained in a rectangle, R, with sides $2R^T$ and $2R_Y^T$ (Fig. 3.2a) or in a circle, C, with radius R_c. (Fig.3.2b)

$$\left.\begin{aligned} E_x^T(x,y) &= 0 \\ E_y^T(x,y) &= 0 \end{aligned}\right\} \text{for } (x,y) \notin A_T \qquad (A.3.1)$$

and

$$E_x^T(x,y) = \mathcal{F}\left\{F_x^T(s_1,s_2)\right\} \qquad (A.3.1)$$

$$E_y^T(x,y) = \mathcal{F}\left\{F_y^T(s_1,s_2)\right\} \qquad (A.3.2)$$

where $\mathcal{F}$ is the double Fourier transform operator.

$$\text{with} \quad P_B(x,y) = \begin{cases} 1 & \text{for} \quad (x,y) \in B \\ 0 & \text{for} \quad (x,y) \notin B \end{cases} \qquad (A.3.3)$$

where B is an arbitrary contour encircling the aperture A_T.

Defining;

$$k_B(s_1,s_2) = \frac{1}{4\pi^2} \iint_B e^{jk(s_1x+s_2y)} \, dxdy \qquad (A.3.4)$$

F_x^T and F_y^T can be expanded in a sampling series as follows [PAP] :

$$F_x^T(s_1,s_2) = \sum_{n=-\infty}^{\infty} \sum_{m=-\infty}^{\infty} c_{nm}^x \, k_B(s_1-mP_1,\ s_2-nP_2) \qquad (A.3.5)$$

$$F_y^T(s_1,s_2) = \sum_{n=-\infty}^{\infty} \sum_{m=-\infty}^{\infty} c_{nm}^Y \, k_B(s_1-mP_1,\ s_2-nP_2) \qquad (A.3.6)$$

where c^x_{nm} and c^y_{nm} are complex coefficients giving the amplitude and phase of the sampled function at the sampling points and P_1 and P_2 refer to the sampling periods given by;

$$P_1 = \frac{\pi}{kR_x^T} \tag{A.3.8}$$

$$P_2 = \pi/kR_y T \tag{A.3.9}$$

If B is the rectangle, R, in Fig. 3.2a, then

$$k_B(s_1,s_2) = \frac{\mathrm{Sin}\left[kR_x^T\ s_1\right]}{kR_x^T\ s_1}\ \frac{\mathrm{Sin}\left[kR_y^T\ s_2\right]}{kR_y^T\ s_2} \tag{A.3.10}$$

On the other hand if B is equal to the circle C in Fig. 3.2b then;

$$k_B(s_1,s_2) = \frac{J_1(kR_c\sqrt{s_1^2 + s_2^2})}{kR_c\sqrt{s_1^2 + s_2^2}} \tag{A.3.11}$$

Hence using Eqs. A.3.5, A.3.6, A.3.10, A.3.11. The sampling expansions for F_x^T and F_y^T given by Eqs. 3.8a,b and 3.11a,b can be obtained.

APPENDIX IV: STATIONARY PHASE EVALUATION OF THE INTEGRAL w.r.t s_1 IN Eq.4.1

In Eq. 4.1, the integral w.r.t s_1 can be epproximated by the first term of a stationary phase evaluation [PAP] . The justification was given in Section 4.1.

s_{1o}, critical point of the first kind occurs at the value of s_1 which maintains;

$$\frac{\partial c'}{\partial s_1} = 0 \rightarrow s_{1o} = s_1 = s_1' = 0 \qquad (A.4.1)$$

And since measurements are done on the $\xi\rho$-plane; $\cos \alpha_j = 0$, $\sin \alpha_j = 1$. Then

$$f_1 \Big|_{s_1=0} = c'^2 \qquad (A.4.2)$$

Then Eq. 4.1 can be written as

$$D(\beta_i) = K_1 \int_{-\infty}^{\infty}\int_{-\infty}^{\infty} (1-s_2'^2)^{\frac{1}{2}} F^s(0,s_2') F_x^T(0,s_2) F_{x'}^R(0,s_2') \, e^{-jk\ell c'} \, ds_1 ds_2 \qquad (A.4.3)$$

Now c' must be expressed in terms of s_1, s_2 and c;

$$\begin{bmatrix} s_1' \\ -s_2' \\ -c' \end{bmatrix} = [R]^{-1} \begin{bmatrix} s_1 \\ s_2 \\ c \end{bmatrix} \qquad (A.4.5)$$

from which one obtains;

$$s_1' = s_1 \tag{A.4.6a}$$

$$s_2' = -\cos\beta_i - s_2 - \sin\beta_i c \tag{A.4.6b}$$

$$c' = \sin\beta_i s_2 - \cos\beta_i c \tag{A.4.6c}$$

Since [PAP];

$$\int_{-\infty}^{\infty} e^{-jk\ell\cos\beta_i\sqrt{1-s_1^2-s_2^2}}\, ds_1 = 2\sqrt{\frac{\pi}{2\left.\frac{\partial^2 c}{\partial s_1^2}\right|_{s_{1o}}}}$$

$$e^{j\frac{\pi}{4}}\ \frac{\left.e^{-jk\ell\cos\beta_i c}\right|_{s_{1o},s_2}}{\sqrt{k\ell\cos\beta_i}} \tag{A.4.7}$$

and since;

$$\left.\frac{\partial^2 c}{\partial s_1^2}\right|_{s_{1o}} = -(1-s_2^2)^{-\frac{1}{2}}$$

$$\int_{-\infty}^{\infty} e^{-jk\ell\cos\beta_i c}\, ds_1 = \sqrt{\frac{\lambda}{\ell\cos\beta_i}}(1-s_2^2)^{\frac{1}{4}}\, e^{j\frac{\pi}{4}}\, e^{-jk\ell\cos\beta_i\sqrt{1-s_2^2}} \tag{A.4.8}$$

Then Eq. A.4.3 reduces to;

$$D(\beta_i) = \frac{K}{\cos\beta_i}\int_{-\infty}^{\infty}(1-s_2^2)^{\frac{1}{4}}(1-s_2'^2)^{\frac{1}{2}}\, F^S(s_2')F_x^T(s_2)F_{x'}^R(s_2')$$

$$e^{-jk\ell\left[\cos\beta_i\sqrt{1-s_2^2}-\sin\beta_i s_2\right]}\, ds_2 \tag{A.4.9}$$

where $$K = \sqrt{\frac{\lambda}{\ell}}\, K_1\, e^{j\frac{\pi}{4}}$$

APPENDIX V: COMPUTER PROGRAM FOR THE SOLUTION OF THE INTEGRAL EQUATION

MAIN PROGRAM

```
C       DETERMINATION OF ANTENNA RADIATION PATTERNS FROM NEAR FIELD
C       MEASUREMENTS USING ANTENNA SYNTHESIS TECHNIQUE
C       INTEGRAL EQUATION SOLUTION METHOD FOR SPECTRUM DETERMINATION
C       DETERMINATION OF UNKNOWN SPECTRUM FROM EXPERIMENTAL RESULTS
        INTEGER*4 KPSI(200)
        COMPLEX*8 COEF(25),F(25,25),TERS(25,25)
        COMPLEX*8 CEY,F4(80),FF4(80),F6,FF6,FPOS(80),FNEG(80)
        COMPLEX*8 REFSG
        COMPLRX*8 F3,FF3
        COMPLEX*8 SIGI(25),SIG2(25),SIGNAL(25)
        COMPLEX*8 CALSP(210)
        COMPLEX*8 REFCO
        REAL*4 POWPT(40)
        REAL*4 PPSI(210)
        REAL*4 VOLT(30)
        REAL*4 POWSP(210)
        REAL*4 WT(80),AW(80),T(80),TT(80),AT(80),X(80),XX(80)
        REAL*4 B(25),BETA(25)
        REAL*4 AMP2(25,3),ANG2(25,3)
        REAL*4 AMP(25,5),ANG(25,5)
C       INITIALIZATION OF CONSTANTS
        PI=3.14159265358979323846264 3
        HPI=0.5*PI
        TWOPI=PI+PI
        PIN=1.0/TWOPI
        KALT=-90
        KSTEP=1
        KMK=178
        RR=4.5
        RT=9.0
        ALAM=30.0/9.87
        AK=TWOPI/ALAM
        JJJ=80
        READ(1,109) (AT(J),AW(J),J=1,JJJ)
        DEL=1.0/6.0
        CEY=CMPLX(0.,1.)
        D=9.0
        AL=55.2
```

```
      RS=13.5
      C1=AK*RS
      C2=AK*D*0.5
      C3=AK*AL
      C4=AK*RR
      C5=4.0*RR/ALAM
      TTCC=RT
      C6=AK*RT
      C7=3.0/(2.0*TTCC)
      C8=C6
      C11=4.0*RT/ALAM
      C12=AK*RT
      RAY=2.0
      CACA=AK*D
      WO=C6
      PER=PI/C6
      W2=TWOPI/PER
      RAT=WO/W2
      II=6
      MM=II
      KIKI=3
      III=2*II+1
      MMM=2*MM+1
C     DETERMINATION OF THE ANGULAR POSITIONS OF THE TRANSMITTING ANTENNA
      DO 27 I=1,III
      AAL=II-1+1
      BBB=AAL*C7
   27 B(I)=ARSIN(BBB)
      DO 37 L=1,III
   37 BETA(L)=(180.0*B(L)/PI
      DO 1881 I=1,III
 1881 READ(1,1883) (AMP(I,J),ANG(I,J),J=1,KIKI)
 1883 FORMAT(6F10.5)
      RAMP=5.0
      DO 1884 I=1,III
      DO 1884 J=1, KIKI
      PRP=(RAMP-AMP(I,J))/20.
 1884 AMP(I,J)=10.0**PRP
      REFAN=0.0
      DO 1885 I=1,III
      DO 1885 J=1,KIKI
 1885 ANG(I,J)=PI*(ANG(I,J)-REFAN)/180.0
      DO 1892 I=1,III
      SIGI(I)=CMPLX(0.0,0.0)
      DO 1892 J=1,KIKI
      ABAB=ANG(I,J)
 1892 SIGI(I)=SIGI(I)+AMP(I,J)*CEXP(CEY*ABAB)
      DO 1895 I=1,III
 1895 SIGNAL(I)=SIGI(I)
      REFSG=SIGNAL(II+1)
      DO 3377 I=1, III
```

```
 3377 SIGNAL(I)=SIGNAL(I)/REFSG
C     PROGRAM TO PRINT OUT THE SIGNAL VALUES
      WRITE(3,3333)
 3333 FORMAT(/10X,4HBETA,30X,6HSIGNAL/)
      WRITE(3,205) (BETA(I),SIGNAL(I),I=1,III)
  205 FORMAT(5X,F15.8,10X,F15.8,2X,F15.8)
      DO 1413 I=1,III
      VOL=REAL(SIGNAL(I)*CONJG(SIGNAL(I)))
 1413 VOLT(I)=10.0*ALOG10(VOL)
      WRITE(3,1415) (VOLT(I),I=1,III)
 1415 FORMAT(30X,F18.8)
      MKMK=91
      READ(1,1883) (POWPT(I),I=1,MKMK)
      REFPT=15.
      DO 6998 I=1,MKMK
 6998 POWPT(I)=POWPT(I)-REFPT
      WRITE(3,6980)
 6980 FORMAT(20X,26HMEASURED AMPLITUDE PATTERN)
      WRITE(3,1883) (POWPT(I),I=1,MKMK)
C     INITIALIZATION OF THE INTEGRAL MATRIX
      DO 7 I=1,III
      DO 7 M=1,MMM
    7 F(I,M)=CMPLX(0.0,0.0)
C     DETERMINATION OF NEW INTEG. LIMITS AND NEW ABCISSA AND NEW WEIGHTS
      DO 81 I=1,III
      BI=B(I)
      A9=DEL
      B9=-DEL
C     CHECK FOR EVANESCENT WAVES
      IF(DEL-(HPI-ABS(BI))) 25,45,45
   45 IF(BI) 22,25,23
   22 A9=HPI+BI
      B9=-DEL
      GO TO 25
   23 A9=DEL
      B9=-HPI+BI
   25 A1=(A9-B9)*0.5
      A2=(A9+B9)*0.5
      DO 31 KK=1,JJJ
      T(KK)=A1*AT(KK)+A2
      TT(KK)=-A1*AT(KK)+A2
   31 WT(KK)=A1*AW(KK)
C     EVALUATION OF SOME OF THE FUNCTIONS IN THE INTEGRAND FOR A
C     SPECIFIC VALUE OF BETA
      DO 61 N=1,JJJ
      F1=COS(T(N))
      FF1=COS(TT(N))
      AF2=SQRT(COS(T(N)-BI))
      AFF2=SQRT(COS(TT(N)-BI))
      F2=AF2*AF2*AF2
      FF2=AFF2*AFF2*AFF2
```

```
      S=SIN(T(N))
      SS=SIN(TT(N))
      F5=1.0+RAY*COS(CACA*S)
      FF5=1.0+RAY*COS(CACA*SS)
      F6=CEXP(-CEY*C3*F1)
      FF6=CEXP(-CEY*C3*FF1)
      E=C4*S
      EE=C4*SS
      H=C5*S
      HH=C5*SS
      F4(N)=COS(E)/(1.0-H*H)
      FF4(N)=COS(EE)/(1.0-HH*HH)
      X(N)=SIN(T(N)-BI)
      XX(N)=SIN(TT(N)-BI)
      FPOS(N)=F1*F2*F4(N)*F5*F6
   61 FNEG(N)=FF1*FF2*FF4(N)*FF5*FF6
C     EVALUATION OF THE INTEGRAL MATRIX
      DO 81 M=1,MMM
      BM=-MM-1+M
C     INTEGRATION BY THE METHOD OF GAUSSIAN QUADRATURE
   82 DO 81 J=1,JJJ
      Z=WO*(X(J)-BM*PER)
      ZZ=WO*(XX(J)-BM*PER)
      IF(ABS(Z)-0.000001) 85,84,84
   85 F3=RAT
      GO TO 86
   84 Y=RAT/Z
      F3=SIN(Z)*Y
   86 IF(ABS(ZZ)-0.000001) 87,88,88
   87 FF3=RAT
      GO TO 81
   88 YY=RAT/ZZ
      FF3=SIN(ZZ)*YY
   81 F(I,M)=F(I,M)+WT(J)*(FPOS(J)*F3+FNEG(J)*FF3)
C     PROGRAM TO PRINT OUT THE INTEGRAL MATRIX
      WRITE(3,444)
  444 FORMAT(/20X,15HINTEGRAL MATRIX/)
      WRITE(3,202)((F(I,M),M=1,MMM),I=1,III)
      CALL INAL1(TERS,F,III)
C     PROGRAM TO PRINT OUT THE INVERSE INTEGRAL MATRIX
      WRITE(3,777)
  777 FORMAT(/20X,27HTHE INVERSE INTEGRAL MATRIX/)
      WRITE(3,202) ((TERS(I,M),M=1,MMM),I=1,III)
C     EVALUATION OF THE UNKNOWN COEFFICIENTS
      DO 7112 I=1,III
 7112 COEF(I)=CMPLX(0.0,0.0)
      DO 7111 I=1,III
      DO 7111 M=1,MMM
 7111 COEF(I)=COEF(I)+TERS(I,M)*SIGNAL(M)*SQRT(COS(B(M)))
```

```
      WRITE(3,1773)
      REFCO=COEF(II+1)
      DO 557 I=1,III
  557 COEF(I)=COEF(I)/REFCO
 1773 FORMAT(/15X,20HCOMPLEX COEFFICIENTS/)
      WRITE(3,679) (COEF(I),I=1,III)
  679 FORMAT(5X,2F15.8)
C     EVALUATION OF UNKNOWN SPECTRUM FUNCTION USING THE FORMULATION
      DO 5991 I=1,KMK
      CALSP(I)=CMPLX(0.0,0.0)
      KPSI(I)=KALT+I)
      PPSI(I)=KPSI(I)
      PSI=(PPSI(I)*PI)/180.0
      DO 5991 M=1,MMM
      CCM=-MM-1+1
      ARG=WO*( SIN(PSI)-CCM*PER)
      IF(ABS(ARG)-0.000001) 15,14,14
   15 FFRRY=RAT
      GO TO 5991
   14 FFRRY=RAT*SIN(ARG)/ARG
 5991 CALSP(I)=CALSP(I)+COEF(M)*FFRRY*COS(PSI)
      DO 599 I=1,KMK
  599 POWSP(I)=REAL(CALSP(I)*CONJG(CALSP(I)))
      ENBUY=POWSP(90)
      DO 2970 I=1,KMK
 2970 POWSP(I)=POWSP(I)/ENBUY
      GUL=0.0
      DO 5888 I=1,KMK
 5888 POWSP(I)=GUL+10.0*ALOG10(POWSP(I))
      WRITE(3,530)
  530 FORMAT(10X,9HANGLE PSI,15X,19HCALCULATED SPECTRUM,15X,14HAMPL.
      SPECTRUM)
      WRITE(3,1030) (PPSI(N), CALSP(N),POWSP(N),N=1,KMK)
 1030 FORMAT(10X,F10.5,12X,F10.5,4X,F10.5,7X,F10.5)
  202 FORMAT(/10(2X,E10.2)/)
  109 FORMAT(F34.32,2X,F35.33)
      STOP
      END
```

SUBROUTINE FOR COMPLEX MATRIX INVERSION

```
      SUBROUTINE INAL1(E,F,N)
      INTEGER*4 I,J,N,L,K,IR(25)
      COMPLEX*8 E(25,25),F(25,25)
      REAL*4 MAX,MAG
      DO 3 I=1,N
      DO 3 J=1,N
    3 E(I,J)=F(I,J)
      L=0
      DO 8 I=1,N
```

```
 8 IR(I)=0
20 MAX=0.0
   DO 14 I=1,N
   IF(I-IR(I))15,14,15
15 MAG=CABS(E(I,I))
   IF(MAG-MAX)14,14,17
17 MAX=MAG
   K=I
14 CONTINUE
   E(K,K)=1.0/E(K,K)
   DO 1 I=1,N
   DO 1 J=1,N
   IF(I.EQ.K.OR.J.EQ.K) GO TO 1
   E(I,J)=E(I,J)-E(I,K)*E(K,K)*E(K,J)
 1 CONTINUE
   DO 2 I=1,N
   IF(I.EQ.K) GO TO 2
   E(I,K)=E(I,K)*E(K,K)
   E(K,I)=-E(K,I)*E(K,K)
 2 CONTINUE
   IR(K)=K
   L=L+1
   IF(L.NE.N) GO TO 20
   RETURN
   END
```

REFERENCES

[BAT] R.H.T.Bates and J.Elliott,"The Determination of the True Side-lobe Level of Long Broadside Arrays from Radiation Pattern Measurements Made in the Fresnel Region", Proc.IEE, 103, c, pp. 307-312, March 1956

[BIC] R.W.Bickmore, "On Focusing Electromagnetic Radiators", Can. J.Phys. 35, pp.1292-1298, 1957

[BIC] R.W.Bickmore, "Fraunhc r Pattern Measurement in the Fresnel Region", Can. .Phys., 35, pp. 1299-1308,1957

[BIR 1] T.Birand, A.Marinçiç, "Correction of Errors in Aerial Far-Field Radiation Pattern Determinations", IEE Elect. Lett. Feb. 1971, 7, No.3, pp. 86-87

[BIR 2] T.Birand, A.Marinçiç, "Antenlerin Radyasyon Diyagramlarının Yeni Bir Metotla Tayini", Elek.Müh.Od.IV. Tek.Kongre Tb. Tb.No.16, ss.174-188, 1970

[BIR 3] T.Birand, "An Investigation about the Measurement of Radiation Patterns of Large Aperture Type Antennas", METU, Elect.Engg.Dept. Interdepartmental Memo No.1

[BIR 4] T.Birand, A.Marinçiç, "Determination of Aerial Far-Field Radiation-Patterns from Near-Field Measurements", IEE Elect.Lett. to be published, June 1971

[BO] M.Born, E.Wolf, "Principles of Optics", Pergamon Press, London, 1965

[BOO] H.G.Booker, P.C.Clemmow, "The Concept of an Angular Spectrum of Plane Waves, and its Relation to that of Polar Diagram and Aperture Distribution", Proc.IEE, Paper No. 992R, January 1950 (97, Pt.III, pp.11-17)

[BRA] B.V.Braude, N.A.Yesepkina, "Measurement of Parameters of Sharply Directive Antennas in the Near Zone by Method of Focusing at Finite Distance", Radio Engg. Elect.Physics. Vol.15, No.6, 1970, pp.956-963 (English Translation)

[BR 1] J.Brown, E.V.Jull, "The Prediction of Aerial Radiation Patterns from Near-Field Measurements", Proc.IEE, Paper No.3649E, Nov. 1961, 108B, pp.635-644

[BR 2] J.Brown, "A Theoretical Analysis of Some Errors in Aerial Measurements", Proc.IEE, 105C, Feb.1958, pp.343-351

[BR 3] J.Brown, "A Generalized Form of Aerial Reciprocity Theorem", Proc. IEE, Mon.301R, April, 1958, 105C, p. 472-475

[CL] P.C.Clemmow, "The Plane Wave Spectrum Representation of Electromagnetic Fields", Pergamon Press, Int.Ser. of Monog. in Electromagnetic Waves, Oxford, 1966

[COL 1] R.E.Collin, F.J.Zucker, "Antenna Theory", Pt.I, Mc Graw-Hill, New-York, 1969

[COL 2] R.E.Collin, F.J.Zucker, "Antenna Theory", Pt.II, Mc Graw-Hill, New-York, 1969

[FRO] C.E.Fröberg, "Introduction to Numerical Analysis", Addison-Wesley Pub.Co., London, 1966

[HAM] M.A.K.Hamid, "The Radiation Pattern of an Antenna from Near-Field Correlation Measurements", IEEE Trans.AP-16, No.3, May 1968, pp. 351-353

[JUL 1] E.V.Jull, "An Investigation of Near-Field Radiation Patterns Measured with Large Antennas", IRE Trans. AP-10, July 1962, pp.363-369

[JUL 2] E.V.Jull, "The Estimation of Aerial Radiation Patterns from Limited Near-Field Measurements", Proc. IEE, Vol. 110, Pt.I, 1963, pp.501-506

[KER 1] D.M.Kerns, "Correction of Near-Field Antenna Measurements Made with an Arbitrary but Known Measuring Antennas", IEE Elect.Lett. 28, May 1970, Vol.6, No.11, pp.346-347

[KER 2] D.M.Kerns, E.S.Dayhoff, "Theory of Diffraction in Microwave Interferometry", J.Res.Nat.Bur.St. 1960, 64B, pp. 1-13

[KER 3] D.M.Kerns, "Recent Experimental Results in Near-Field Antenna Measurements", IEE Elect.Lett., 28 May 1970, Vol. 6, No.11, pp.349-351

[KUZ] A.D.Kuz'min, A.E.Salomonovich, "Radioastronomical Methods of Antenna Measurements", Academic Press, London, 1966

[MAR] W.W.Martin, "Computation of Antenna Radiation Patterns from Near-Field Measurements", IEEE Trans. AP.15, March 1967, pp.316-318

[MART] V.V.Martsafey, "Measurement of Electrodynamic Antenna Parameters by the Method of Synthesized Apertures", Radio Engg. Electronic Physics, Vol.13, No.12, 1968, pp.1869-1873 (English Translation)

[PAP] A.Papoulis, "Systems and Transforms with Applications in Optics", Mc Graw-Hill, New York, 1968

[RAM] J.F.Ramsay, "Fourier Transforms in Aerial Theory", Marconi Rev. Parts I-VI, Issue No. 63-69, 1946

[SIL] S.Silver, "Microwave Antenna Theory and Design", Dover Publications, New York, 1965

[ST] J.A.Stratton, "Electromagnetic Theory", Mc Graw-Hill, New-York 1941

[TSE] V.B.Tseytlis, "Measurement of Parameters of Highly Directive Reflector Antennas by the Method of Focusing at a Finite Distance", Radio Engg.Elect. Physics, Vol.13, No.12, 1968 (English Translation)

[TOK] Y.Tokad, "Private Communication", METU Dept. of Elect. Engg. 1971

[WO 1] G.A.Woonton, J.A.Carruthers, "Indoor Measurement of Microwave Antenna Radiation Patterns by Means of a Metal Lens", Journ. of App.Phys. 1950, Vol.21, pp.428-430

[WO 2] G.A.Woonton, J.A.Carruthers, H.A. Elliott, E.C.Rigby, "Diffraction Errors in an Optical Measurement at Radio Wavelengths", Journ. of App. Phys. Vol. 22, 1951, pp.390-397

LIST OF EQUIPMENT USED

Quantity	Equipment
1	Reflex Klystron, X13(8.1-12.4 GHz) Thomson Varian
1	Power Supply and Modulator, Klystron Power Unit Mk.III W.H.Sanders (lectronics) Ltd.
1	Isolator, 40 db isolation, 1db insertion loss, Melabs, Model RX-10
1	Calibrated Variable Attenuator, Hewlett-Packard, Model X382A
1	Calibrated Variable Phase Shifter, Hewlett-Packard, Model X885A
1	Frequency Meter, Hewlett-Packard, Model X532B
1	Cross Coupler, Sanders, DC 16/20, 319
2	Variable Attenuator, PRD, Serial:3302
2	Isolators, Kearfott
1	Directional Coupler (20 db), Hewlett-Packard, Model X752D
1	Tunable Crystal Detector, Philips, PP4221X
1	Matched Termination, Sanders, MTS16
1	3-Screw Tuner, Sanders, ST16
3	Adapter, Hewlett-Packard, X281A
1	Crystal Detector, Hewlett-Packard, X424A
1	Variable Impedance, Sanders, VI16
1	1.5 meter Flexible Coaxial Cable, Amphenol, RG214/u,21-780
1	Standing Wave Ratio Meter, Hewlett-Packard,415E
1	Crystal Detector Mount, AEL,Mod.CNB101A
1	Pyramidal Horn, Sanders, X16C
1	Coaxial Rotary Joint, General Radio, Type 847

ALICI ANTENLER
VERİCİ ANTENLER
MİKRODALGA ANTENLER
ANTEN IŞIMA ÖRÜNTÜLERİ - UZAK ALAN
ANTEN IŞIMA ÖRÜNTÜ ÖLÇÜMÜ - YAKIN ALAN
İNTEGRAL DENKLEMLERİ - ÇÖZÜM
BİLGİSAYAR PROGRAMLARI
ELEKTROMANYETİK DALGA İLETİMİ
ELEKTROMANYETİK ALANLAR
ELEKTRİK ALANLAR
ANTEN TEORİSİ
SPEKTRAL ANALİZ
SAYISAL ANALİZ
HATA DÜZELTME
FOURIER DÖNÜŞÜMÜ
ÖLÇME DÜZENEKLERİ